Modeling the functional coupling between 3D chromatin organization and epigenome

Cédric Vaillant*[1] and Daniel Jost†[2]

[1] *Univ Lyon, ENS de Lyon, Univ Claude Bernard, CNRS, Laboratoire de Physique, Lyon, France*

[2] *Univ Grenoble Alpes, CNRS, Grenoble INP, TIMC-IMAG, Grenoble, France*

abstract

In this chapter, we present our recent theoretical developments about the spatio-temporal dynamics of eukaryotic chromosomes. As physicists, our objective is to provide some universal principles driving chromatin folding. In particular, we focus on the functional compartmentalization of the genome into active versus inactive (epi)genomic domains. First, by introducing a block copolymer framework with self-attraction between loci sharing the same chromatin state, we show that this spatial segregation can be accounted by a microphase separation of the epigenome, characterized by dynamical and stochastic clustering. Then, we address the fundamental question of how chromosome organization may contribute to epigenome regulation by introducing the "nano-reactor" hypothesis that proposes that 3D compartments may provide a favorable micro-environment for robust genome regulation. As an illustration, we present the Living Chromatin model that combines the modeling of the stochastic epigenomic assembly with the modeling of chromatin fiber dynamics. We show how the crosstalk between spatial condensation and long-range *trans* spreading mechanisms may strongly favors the formation and maintenance of stable epigenomic domains. All these results suggest that epigenome is a main driver of 3D chromosome organization that in turn contributes to a robust and efficient epigenomic regulation.

I. INTRODUCTION

Proper 3D organization and dynamics play essential roles in the good operation of many biological processes and are involved in functions as varied as enzymatic activity by well-folded proteins, cell motility generated by architected dynamical cytoskeletons or organ formation by spatially- and temporally-controlled gene expressions. Although acting on various scales ranging from molecules to organisms, the regulation of such structural and dynamical properties mainly originates from molecular mechanisms. How such microscopic actions are coupled to collectively generate large-scale functions is a long-standing, open question.

In this context, understanding how the genome self-organizes inside the cell nucleus is one of the major challenges faced in recent years by biology. Thanks to the recent development of new experimental techniques, especially chromosome conformation capture (Hi-C) technologies [3], supported by parallel confocal and superresolution microscopy studies [4], major progresses have been realized in our understanding of the hierarchical chromosome organization: from the local packaging of DNA into a polymer-like chromatin fiber to large-scale compartmentalization of transcriptionally-active or inactive genomic regions (Fig.1). Briefly (see chapter XXX of the present book

* email: cedric.vaillant@ens-lyon.fr
† email: daniel.jost@univ-grenoble-alpes.fr

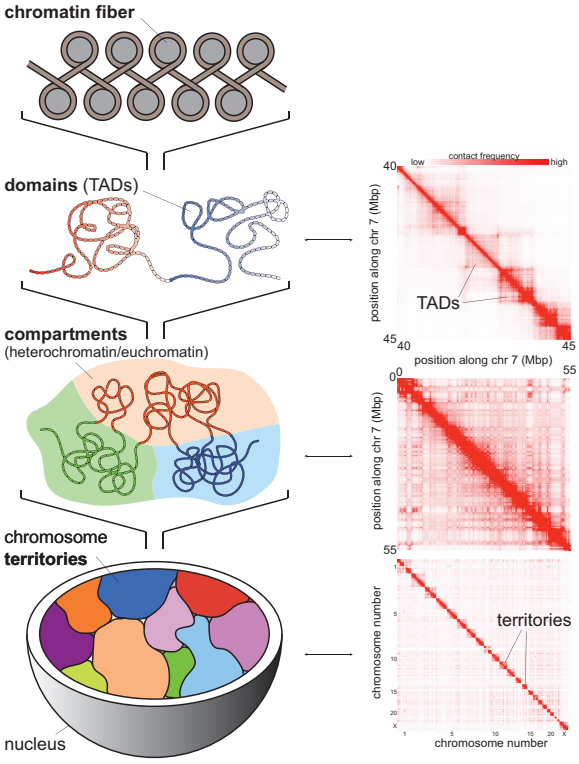

FIG. 1: **Chromosome hierarchical folding**. (Left) Scheme of the multi-scale organization of chromosome during interphase. (Right) Hi-C maps for GM12878 cell line at different resolutions [1] plotted using HiC JuiceBox [2].

for a detailed review), chromosome is locally partitioned into conserved consecutive 200nm-sized contact domains, the so-called topologically-associating domains (TADs), representing the partial folding of kilobasepair- (kbp) to megabasepair-(Mbp) long genomic regions [5–7]. TADs are defined as highly self-contacting portions of the genome: a sequence inside a TAD has a higher probability to contact sequences inside the same TAD than sequences in neighboring TADs at the same linear distance along the genome, thereby segmenting chromosomes into 3D domains. At the Mbp level, contact maps display a cell-type specific checkerboard pattern: parts of the genome that share the same transcriptional activity tend to colocalize forming nuclear compartments [1, 7–9], quantifying the older qualitative observations of nuclear organization made by electron microscopy [10]. Inactive regions, the so-called heterochromatin, are preferentially localized at the nuclear periphery while active regions, the so-called euchromatin, occupy more central positions. Reversely, genomic regions that preferentially localize closed to the nuclear membrane, the so-called lamina-associated domains (LADs), are mainly heterochromatic [11–13]. At the nuclear level, Hi-C maps [8] confirm that chromosomes occupy distinct spatial territory and do not mix [14, 15]. While the vast majority of Hi-C data is obtained at the population level, very recent single-cell Hi-C experiments [16–19], complemented by superresolution microscopy [7, 20, 21], have highlighted the strong stochasticity of chromosome folding suggesting that chromatin is highly dynamical and plastic along the cell cycle and during differentiation. However, direct *in vivo* characterization of chromatin motion is still challenging [22]. Only few studies have successfully tracked fluorescently-labeled loci during relatively long time windows up to few minutes [23–28]. They complete the picture of a fluctuating organization whose dynamics is strongly dependent on transcriptional activity.

An increasing number of experimental evidence suggests that genome 3D organization and dynamics adapt to

nuclear functions and may play a decisive role in gene regulation and disease [29–31]. Most characterized promoter-enhancer interactions occur within the same TAD [32, 33], suggesting that TADs allow insulation of promoters from enhancers located in neighboring TADs. Disruption of a boundary between two consecutive TADs may cause gene misregulation leading to malformations or cancers [34, 35]. Current experimental knowledge has suggested several molecular mechanisms involved in the local and higher-order organization of chromosome [36, 37]. Statistical positioning inside the nucleus and formation of active/inactive compartments are putatively driven by chromatin-binding proteins that are known to bind at specific positions along the genome and that have the capacity to self-interact [38–41] or to interact with membrane proteins [42]. TAD formation is partly associated to the translocation along the genome of protein complexes [43–45], cohesin or condensin rings, that extrude chromatin loops and stop at specific, properly-oriented sites where a known transcription factor, the insulator CTCF, bind [1, 46].

However, investigating experimentally how such molecular mechanisms precisely act and cooperate together to control the dynamics and 3D multi-scale folding of the genome is very challenging and is limited by the experimental difficulty to capture the dynamical stochastic evolution of chromosomes. In the recent years, to partly circumvent such limitations, physical models have been instrumental in simulating chromosome folding and in testing different molecular mechanisms (see [36, 47–50] for reviews and other chapters in the present book). In this chapter, we review our current efforts to understand the functional coupling between the 3D dynamical organization of chromatin and the 1D segmentation of genome into active and inactive domains using polymer and statistical physics modeling.

II. 3D CHROMATIN ORGANIZATION AND EPIGENOMICS

All the cells of a multi-cellular organism contain the same genetic information but may have different shapes, physiologies, metabolisms or functions depending on the cell types, tissues, environments or differentiation stages. These differences are mainly due to the context-dependent differential regulation of gene expression. Gene expression is regulated at various levels from the binding of transcription factors to the post-translational modifications of the synthesized proteins. Among these different layers of regulation, the modulation of accessibility and specificity of regulators to their cognate DNA sites plays a central role. Locally, the chromatin is characterized by many features like nucleosome positioning, biochemical modifications of DNA and histones tails or insertion of histone variants, that contribute significantly to controlling such modulation. In the past decades, advances in sequencing technologies have allowed to characterize in details the genomic profiles of various histone modifications or chromatin-binding proteins, shedding light on the association between these so-called epigenomic marks and gene regulation. In many eukaryotes from yeast to human [51–54], statistical analyses of these patterns along the genome showed that chromosomes are linearly partitioned into 1D cell-type-specific epigenomic domains that extend from few kilobases to megabases and are characterized by the local enrichment of specific epigenomic marks. While based on dozens of profiles, these studies have identified only a small number of main chromatin types for the epigenomic domains (typically 4 to 10, depending on the resolution): (1) euchromatic states, containing constitutively-expressed or activated genes and enhancers, and heterochromatic states covering (2) constitutive heterochromatin associated with HP1 proteins and H3K9me3 mark and mainly found in repetitive sequences such as (peri)centromeres, (sub)telomeres or transposable elements, (3) facultative heterochromatin associated with Polycomb (PcG) complexes and H3K27me3 mark tagging silent -developmentally-regulated - genes, and (4) a less epigenomically-defined repressive state, the so-called black

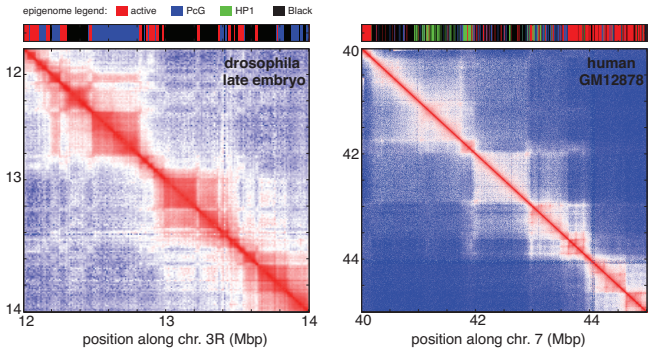

FIG. 2: **Coupling between epigenome and contactome**. (Left) Hi-C map of a 2 Mbp-long genomic region of drosophila chromosome arm 3R, obtained for late embryos [56]. On top, we plot the local epigenomic state (see color legend) as obtained by Fillion et al [52] for the embryonic cell line Kc167 (for simplicity we merged the two originally-defined active states into one single active state). (Right) Hi-C map for a 5 Mbp-long genomic region of human chromosome 7 obtained for the GM12878 cell line [1]. Epigenomic states were taken from Ho et al [51]. For simplicity, we clustered the 16 originally-defined states into the 4 standard chromatin types.

or null or quiescent chromatin, that encompasses gene desert, or genes only expressed in few tissues. Typically, in higher eukaryotes, $\sim 20-30\%$ of mappable genomic loci (excluding telomeres and centromeres) correspond to active states, $\sim 5-10\%$ HP1-like states, $\sim 10-20\%$ PcG-like states and $\sim 40-50\%$ quiescent states, the exact repartition depending on organisms and cell types [55].

From the early studies of nuclear organization made by conventional or electron microscopy [10], it was clear that the active and inactive parts of the genome phase-segregate into (micro)-compartments, heterochromatin localizing mainly at the nuclear periphery and around nucleoli and euchromatin being more internal. Recent developments in Hi-C and superresolution techniques have allowed to quantify in more details the relation between spatial organization and epigenomics [1]. At large-scale, for a given cell-type, statistical analyses of specific checkerboard patterns observed in Hi-C maps (Fig.1) showed that genomic loci can be clustered into two groups, the so-called A and B compartments [8, 57]: the contact frequency from sequences of the same group (A *vs.* A or B *vs.* B) is stronger (~ 2 fold) than from sequences in different ones (A *vs.* B). Genomic regions corresponding to A compartment are gene-rich and are associated with histone marks specific to active genes. In contrast, loci belonging to B compartment harbor a weak gene density and contain more repressed histone modifications. These compartments can be subdivided into subgroups that exhibit peculiar contact patterns and that correspond to different epigenomic states [1]. Reciprocally, epigenomic domains (as defined above) contact more frequently domains of the same chromatin type than domains with different states [56]. Recent single-cell Hi-C experiments [17–19] and high-resolution imaging of multiple probes on the same chromosome [20, 21] have confirmed that loci sharing the same epigenomic content tend to colocalize inside the nucleus. Altogether, these observations demonstrate the large-scale clustering of functionally-similar genomic loci.
At the sub-Mbp scale, TADs are also significantly correlated with epigenomic domains [51, 55, 58] (Fig.2). In drosophila, positioning of TADs along the genome displays strong similarity with the locations of epigenomic domains [55, 58, 59]: loci within the same TAD tend to have the same chromatin state (Fig.2, left), boundaries between TADs are enriched in active marks, and the large-scale checkerboard pattern emerges from long-range interactions between TADs of the same chromatin type [56]. Recent superresolution microscopy of individual TADs showed

that the epigenomic state also impacts the local 3D chromatin compaction: active TADs being less compact than black/quiescent and PcG-associated TADs [7, 21], confirming the observations that more Hi-C contacts are observed in inactive domains [60]. All this suggests that, in drosophila, TAD formation is strongly associated with epigenomic domains. In mammals, TADs are also significantly associated with the local chromatin state [51, 55] even if the correspondence between TAD and epigenomic segmentations is less clear (Fig.2 right). TAD boundaries are mainly characterized by the binding of insulator proteins like CTCF and do not necessarily reflect the frontiers between different epigenomic domains. Recent experimental and modeling works suggest that, in mammals, TADs might emerge from the coupled action of CTCF-cohesin-mediated mechanism (see the presentation of the loop extrusion model in [43, 44] and in Chapter XX of the present book) and of epigenomically-associated mechanism as in drosophila [61, 62].

Altogether, these results highlight the strong interplay between the *1D* segmentation of the genome into epigenomic domains, the so-called epigenome, and the *3D* compartmentalization of chromosomes into contact domains, the so-called "contactome". This crosstalk is now well documented and has inspired numerous statistical works inferring various 3D organization features like TAD or compartments from epigenomic data [58, 63, 64] or using the 3D contact information to better understand various aspects of gene regulation [65]. However, the *mechanistic* foundations of such coupling are still unclear. In particular, to what extent epigenomically-associated mechanisms drive chromosome organization? What is the role of this non-random 3D organization in the establishment and maintenance of a stable epigenomic information?

In the next, we will present and discuss how we addressed the former question using polymer physics in the context of chromatin folding in drosophila (Section III) and how we formalized the latter question with theoretical modeling (Section IV).

III. EPIGENOME-DRIVEN PHASE SEPARATION OF CHROMATIN

The observed correlations between epigenome and contactome suggest the existence of epigenomic-specific mechanisms playing major roles in chromatin folding. Actually, there is an increasing number of experimental evidence showing that chromatin-binding proteins associated to specific epigenomic domains possess the molecular capacity to interact or oligomerize, hence promoting directly or effectively physical bridging between genomic loci of the same chromatin type. Indeed, heterochromatin-associated factors like PcG or HP1 display structural domains (respectively sterile alpha motif (SAM) domains or chromodomains (CD)) that may favor multimerization [38, 39]. In particular, very recent experiments showed that human and drosophila HP-1 can self-interacts, leading eventually to a liquid-like phase separation *in vitro*, in absence of chromatin and to the formation of *in vivo* heterochromatic compartments [40, 41]. Similarly, mutualization of transcription machinery resources or DNA looping mediated by promoter-enhancer interactions may also lead to effective attractions between active loci [66–68]. Black/quiescent chromatin is often associated with lamins or is enriched in histone H1 that may also promote binding. In addition, *in vitro* experiments have demonstrated that two nucleosomes may interact directly and that such interactions are sensitive to biochemical modifications of histone tails [69, 70].

All this suggests that the heterochromatin/euchromatin phase separation is driven by specific short-range interactions mediated by epigenomic markers like histone modifications or chromatin-binding proteins.

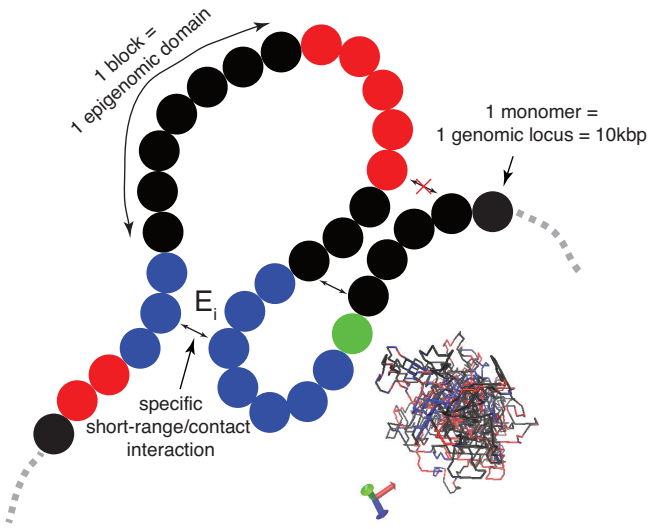

FIG. 3: **Block copolymer model**. Each monomer represents a given genomic locus. One block corresponds to one epigenomic domain. Pairwise interactions between monomers depend on the local epigenomic state. (Bottom right corner) Snapshot taken from a kinetic Monte-Carlo simulation of the block copolymer model of drosophila chromosome 3R.

A. Block copolymer model

To formalize and test this hypothesis, we developed a general framework by treating chromatin as a block copolymer (Fig.3), where each block corresponds to an epigenomic domain and where each monomer interacts preferentially with other monomers of the same chromatin type. While being generic, we focused our approach on chromatin folding in drosophila where the coupling between epigenome and contactome is very strong. Similar approaches have been also applied to mammals by other groups and will be discussed below (Sec.III F).

More specifically, we modeled chromatin as a semi-flexible, self-avoiding, self-interacting polymer [60, 71–73]. A chain corresponding to a given genomic region is composed by N monomers, each representing n bp. Each bead m is characterized by its epigenomic state $e(m)$. We limit our analysis to the four major classes of chromatin state described above (active, PcG, HP-1 and black/quiescent). A long epigenomic domain will thus be represented by a block of consecutive monomers all sharing the same state. Beads of the same epigenomic state may specifically interact via short-range, transient interactions. The full dynamics of the chain is then governed by two contributions: (i) bending rigidity and excluded volume describing the "null" model of the chain, and (ii) epigenomics-mediated attractive interactions.

By definition, this model belongs to the generic family of block copolymers. In the past decades, this wide class of models has been extensively studied in physics and chemistry, mainly to characterize the phase diagram of melts of short synthetic chains composed by few blocks arranged either periodically or randomly [74]. However, the properties of such framework applied to long polymers (the chromosomes) with many block of various sizes (the epigenomic domains) is poorly characterized.

B. Simulation methods

In recent years, we have developed several methods to investigate the behavior of the block copolymer model of chromatin. From self-consistent Gaussian approximations allowing to efficiently access the steady-state behavior of short chains [71, 72] to more detailed numerical simulations of the chain dynamics [60, 73]. In this chapter, we will focus on our most recent results using simulations of long chains, recapitulating all our previous findings.

The polymer is modeled as a self-avoiding walk on a Face Centered Cubic (FCC) lattice to allow maximal coordination number (= 12). The energy of a given configuration is given by

$$H = \frac{\kappa}{2}\sum_{m=1}^{N-1}(1-\cos\theta_m) + \sum_{l,m} U_{e(l),e(m)}\delta_{l,m}. \quad (1)$$

The first contribution accounts for the local stiffness of the chain with κ the bending rigidity and θ_m the angle between bond vectors m and $m+1$. The second contribution accounts for epigenomic-driven interactions with $\delta_{l,m} = 1$ if monomers l and m occupy nearest-neighbor (NN) sites on the lattice ($\delta_{l,m} = 0$ otherwise), and $U_{e,e'}$ the strength of interaction between a pair of spatially neighbor beads of chromatin states e and e'. For simplicity, we will assume that interactions occur only between monomers of the same chromatin state ($U_{e,e'} = 0$ if $e \neq e'$) and that the strength of interaction (that we note E_i) is the same whatever the chromatin state ($U_{e,e} \equiv E_i$ for all e). Confinement and effect of other chains are accounting by using periodic boundary conditions. Dynamics of the chain follows a kinetic Monte-Carlo (KMC) scheme with local moves developed by Hugouvieux and coworkers [75]. This scheme allows at most two monomers to occupy the same lattice site if and only if they are consecutive along the chain. One Monte Carlo step (MCS) consists of N trial moves where a monomer is randomly chosen and displaced to a nearest-neighbor site on the lattice. Trial moves are accepted according to a Metropolis criterion applied to H and if the chain connectivity is maintained and the self-avoidance criterion is not violated. These simple rules allow efficient simulations of reptation motion in dense - topologically constrained - systems, while still accounting for the main characteristics of polymer dynamics like polymer connectivity, excluded volume, and non-crossability of polymer strands. More details on the lattice model and KMC scheme can be found in [60, 73, 75].

As explained in chapter XX of the present book, chromosomes are intrinsically long, topologically-constrained - so-called crumpled -polymers. These constraints have a strong impact on the dynamics of the chain and leads to peculiar structural and dynamical scalings[50, 76, 77] different from classical Rouse or worm-like chain models [78]. Recently, we derived a coarse-graining strategy [73] that accounts properly for this regime and establishes an intelligible method to fix some model parameters (bending rigidity and number of sites in the simulation box) at a desired resolution. This strategy allows simulating long chromatin fragments ($N \times n \approx 20$ Mbp) with high numerical efficiency while conserving the structural and dynamical properties of the chain emerging from steric entanglement [73]. In the next, we will describe results obtained at a genomic resolution of $n = 10$ kbp and a spatial resolution of ~ 100 nm (the distance between NN sites on the lattice) which are both typical resolutions achieved in standard Hi-C and microcopy experiments.

For a given set of parameters, the time-unit in our simulations was determined by mapping the predicted time-evolution of the mean-squared displacement (MSD) of individual loci to the typical experimental relation: MSD (in μm^2) $\sim 0.01 t^{0.5}$ (with time t in second), observed in higher eukaryotes [23, 26–28]. For standard parameter values used in the next, we found that 1 MCS, the temporal resolution of the model, corresponds to $\sim 0.01 - 0.05$ sec.

C. Phase-diagram of the model: towards (micro)phase separation

To illustrate the behavior of the model, we simulated the dynamical folding of a 20 Mbp-long region of drosophila chromosome arm 3R (position $7-27$ Mbp) for various values of E_i, the only free parameter of the model. Starting from random, compact, unknotted configurations resembling post-mitotic structures of chromosomes [79], we tracked, for thousands of different trajectories, the dynamical evolution of polymer conformations during 20 hours of "real" time, the typical duration of a cell cycle.

In Figure 4 A, we plotted the predicted Hi-C maps for a population of unsynchronized cells as in standard Hi-C experiments, ie averaged over one cell cycle. At very weak interaction strengths, the polymer behaves as a (nearly) homogeneous chain driven mainly by steric interactions. It has the full characteristics of a crumpled polymer, as explained in details in chapter XX of the present book. As $|E_i|$ is increased, the heteropolymeric nature of the system becomes apparent at the local and large scales. Locally, the contact probability between monomers of the same block increases (Fig.4A) and the spatial size of individual epigenomic domains (quantified by the square radius of gyration) decreases (Fig.4 B, squares), leading to the formation of more or less compact TADs, depending on the strength of E_i and the linear size of the block (longer block being more compact at the same interaction strength, data not shown, see [60, 80]). Similarly, at large scale, long-range contacts between TADs of the same chromatin type are enhanced and TADs of different types phase-segregate, leading to a typical checkerboard pattern in predicted Hi-C maps. Structurally, as the strength of interaction augments, monomers of the same epigenomic state aggregate and form larger and more compact distinct 3D domains (Fig.4C,D). At high E_i values, this is characteristics of a microphase separation as typically observed in short block copolymer melts [74]. Interestingly, the formation of such large-scale compartmentalization impacts strongly the local organization. Indeed, the compaction of individual TADs is significantly lower in presence of long-range contacts than in situations where we only authorize the internal folding of epigenomic domains (circles in Fig.4 B): in partial or full (micro)phase separation, TADs of the same chromatin type dynamically merge into big 3D clusters allowing conformations of an individual epigenomic block to be more expanded. Such property explains also why, for similar block sizes, the PcG domain in Fig.4B (blue squares) is more compact than the active (red) and the black domains: in drosophila, large PcG domains are mainly far from each other along the genome, hence very close to the isolated case, while active and black domains are surrounded by much more domains of the same type.

D. Comparison to experiments

At each investigated value of E_i, we computed the Pearson correlation between the predicted contact map and the corresponding experimental data obtained by Sexton et al [56] on late drosophila embryos. The correlation was maximal (0.86) for $E_i = -0.1 k_B T$. Figure 5A illustrates the very good agreement between both maps at the TAD and Mbp levels. For the predicted and experimental maps, we computed the scores on the first principal component of the normalized contact frequency matrix $\bar{C}$ defined as $\bar{C}(l,m) = C(l,m)/P_c(|l-m|)$ with $C(l,m)$ the contact frequency between loci l and m, and $P_c(s)$ the average contact frequency between two loci separated by a genomic distance s. For one profile, loci with similar scores tend to belong to the same spatial A/B compartment [8, 57]. Both profiles (Fig.5A) are strongly correlated (Spearman correlation = 0.74) illustrating how well the checkerboard pattern is

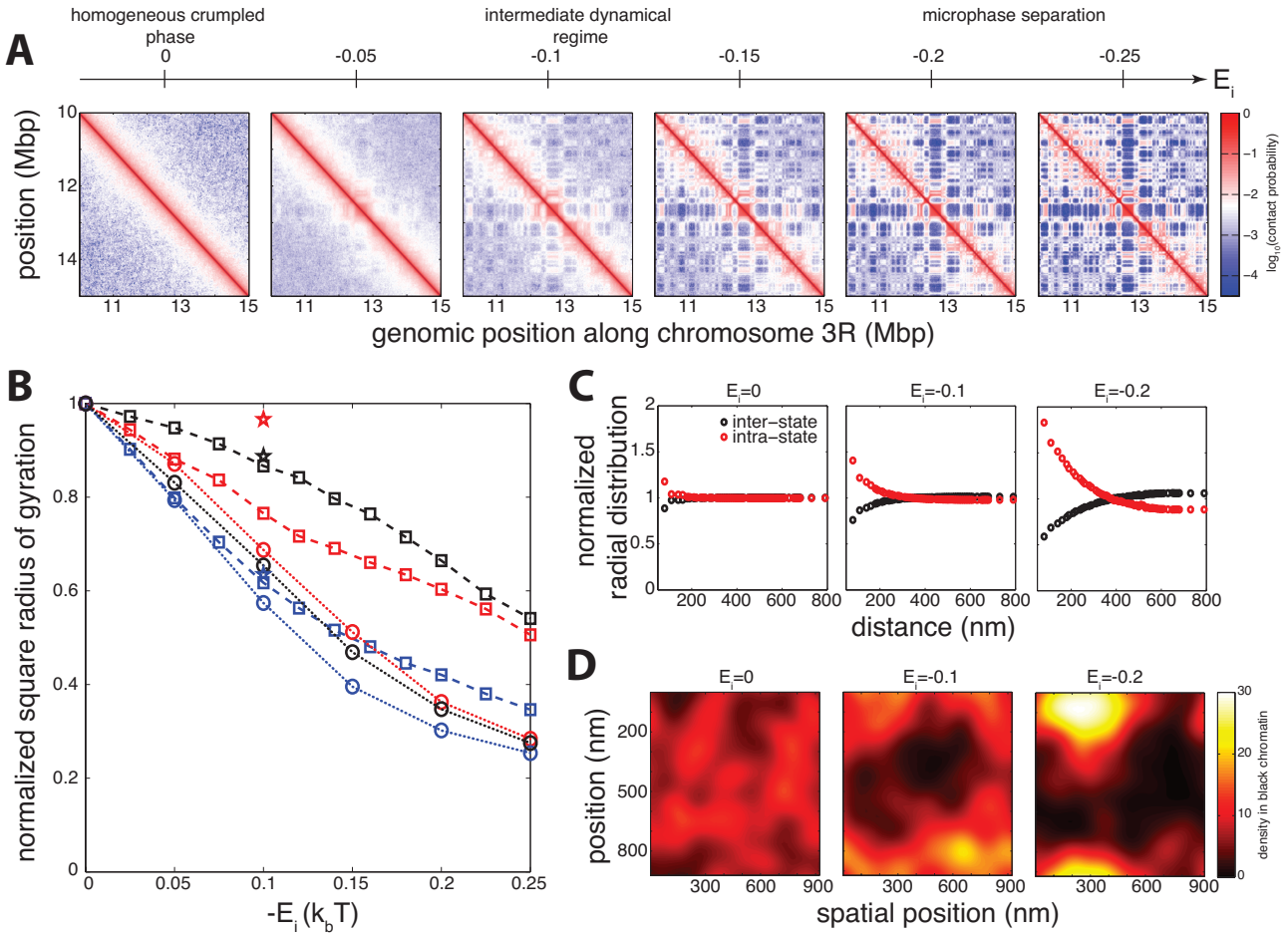

FIG. 4: **Phase diagram of the block copolymer model**. (A) Predicted Hi-C maps for a 20 Mbp-long region of drosophila chromosome 3R for increasing strengths of attraction E_i (in k_BT-unit). (B) Evolution of the square radius of gyration (defined as $1/(2N^2)\sum_{l,m}(\mathbf{r_l}-\mathbf{r_m})^2$, an estimator of the average square 3D size of a domain) as a function of E_i for 3 large epigenomic domains (red squares: 1 active domain of size 280 kbp; blue squares: 1 PcG of size 330 kbp; black squares: 1 black/quiescent of size 290 kbp). Data were normalized by the corresponding values in the homogeneous case ($E_i = 0$). Circles correspond to situations where we authorized interactions *only* between monomers of the same epigenomic *domain* (no long-range interaction between TADs of the same state). Stars described the case where the specific interaction strength between active monomers was set to zero (PcG, HP1 and black monomers can still interact with monomers of the same type with $E_i = -0.1$). (C) Probability to find a monomer of the same (red circles) or different (black circles) epigenomic state at a given distance from a reference monomer (radial distribution), for three different values of E_i. Data were normalized by the corresponding probability to find a monomer of any state. (D) Typical examples of the volumic density in black monomers in a 2D slice of the simulation box, for three different values of E_i.

reproduced (positions and intensities) by the block copolymer model. Given the simplicity of the model, it is quite remarkable, suggesting that epigenomic-driven forces are main players of the chromosome folding in drosophila.

Interestingly, experimental data locate at an intermediate position in the phase diagram (Fig.4 A) between the homogeneous - crumpled - phase and the full microphase separation. Interaction strength is weak, TADs are only partially collapsed (Fig.4 B) and spatial compartments are dynamic and stochastic structures (see below) of typical

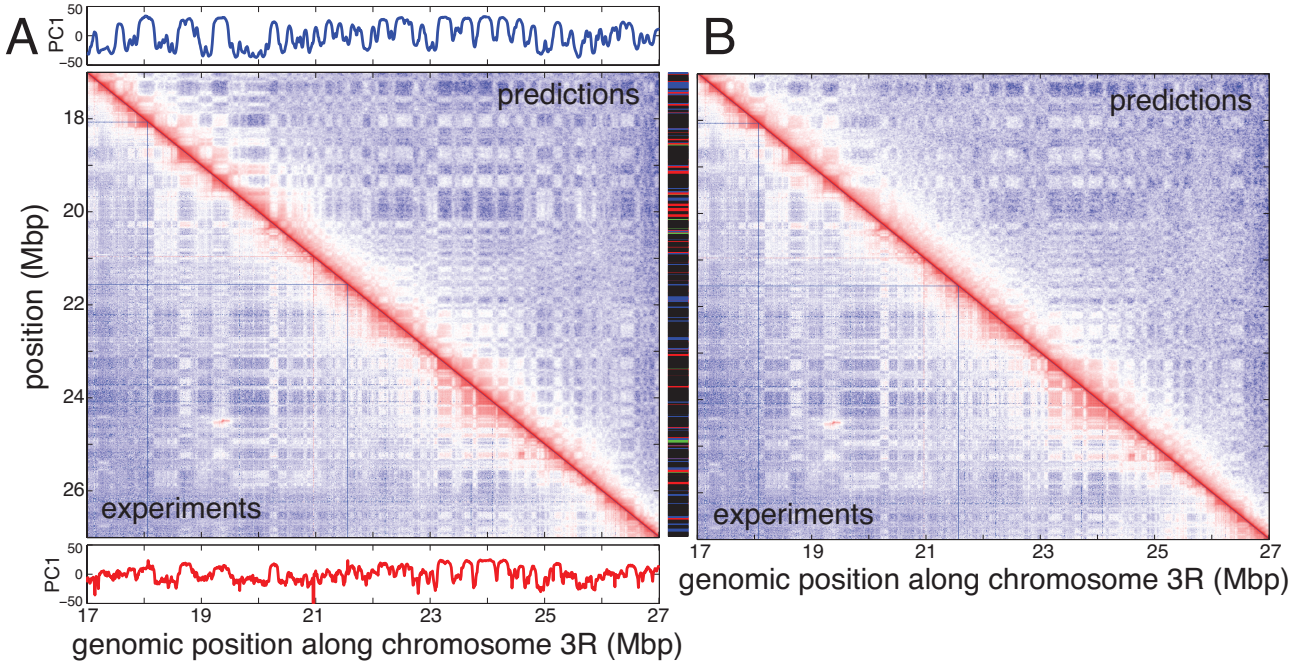

FIG. 5: **Comparison between experimental and predicted data**. (A) (Middle) Predicted ($E_i = -0.1k_bT$, upper triangular part) versus experimental (lower triangular part) Hi-C maps for a 10 Mbp region. Experimental data from [56]. Same color code as in Fig.4A. Experimental data divided by a factor 2500 to linearly adjust both scales. (Top, Bottom) A/B compartment analysis (see text) of the predicted (top) and experimental (bottom) Hi-C maps: loci with a negative (resp. positive) scores on the first principal component (PC1) belong to the A (resp. B) compartment. (B) Same of (A) but for the case where the specific interaction strength between active monomers was set to zero (PcG, HP1 and black monomers can still interact with monomers of the same type with $E_i = -0.1$).

size $\sim 200 - 300$ nm (Fig.4 C,D). The model predicted that PcG domains are more compact than black domains, in qualitative agreement with recent measurements in flies of the radius of gyration [7] and of the end-to-end-distances of various epigenomic domains [21]. This means that the observed differences in compaction between PcG and black domains can be explained in great part by differences in the linear organization of epigenomic blocks along the genome, and not necessarily by differences in interaction strength as stated in [7]. However, as it is, the model failed to predict that active domains are less compact that heterochromatin domains [7]. This discrepancy suggests that interactions between active monomers may be lower or dispensable to describe chromatin folding in drosophila. Fig.5B illustrated indeed that setting the interaction strength between active beads to zero while keeping $E_i = -0.1$ for the others, still allows to globally well describe the Hi-C map (Pearson correlation = 0.86, with a weak loss in phase-segregation) while improving predictions for the compaction of active domains that are now less compact than heterochromatic regions (stars in Fig.4 B). This suggests that in drosophila, the euchromatin/heterochromatin compartmentalization is mainly driven by the interactions between the dominant black/quiescent - heterochromatic - loci. The formation of the A (euchromatic) compartment is just a byproduct of these direct interactions: small active regions are expelled at the periphery of the heterochromatic (micro)compartments leading also to preferential - effective - interactions between active sites.

Looking carefully at the predicted and experimental Hi-C maps, we observed however several discrepancies between

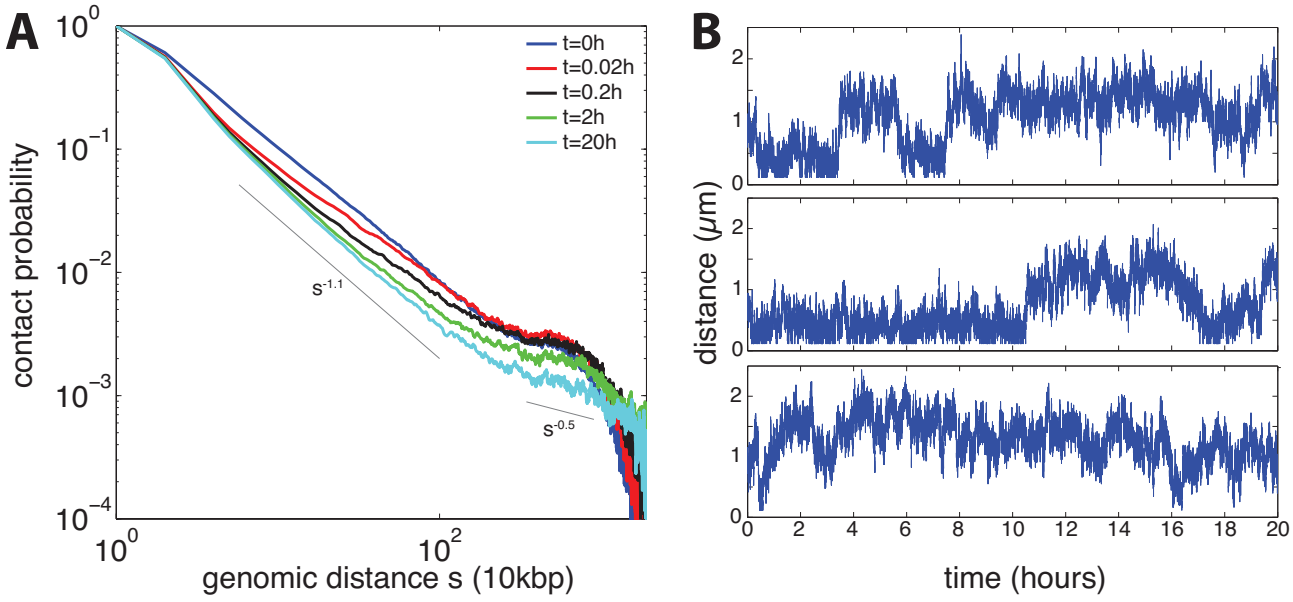

FIG. 6: **Dynamical chromatin folding**. (A) Average contact probability between two loci as a function of their relative genomic distance along the genome predicted by the block copolymer model ($E_i = -0.1k_bT$) at different time points during one cell cycle. (B) Examples of the time evolution of the distance between two loci of the same epigenomic state separated by 3 Mbp along the genome.

both maps, suggesting missing ingredients in the model. For example, the model predicted spurious or misses TADs or long-range contacts between TADs. This could be due to a wrong annotation of the local epigenomic state (we use epigenomic data from an embryonic cell line while Hi-C data were obtained on whole embryos) or the existence of specific interactions driven by other biological processes not accounted in the model like promoter-enhancer interactions. Refining the model to account more precisely for the local epigenetic content (for example for the relative levels of histone modifications or chromatin-binding proteins) or differences in interaction strengths between different states would certainly lead to a better correspondence. We also observed that TADs are more sharply defined in the experiments, particularly in the corners of large TADs. This might be the results of pairing between homologous chromosomes, a phenomenon commonly found in Diptera [81] and not accounted by the model, or of the presence of extra cis-interacting mechanisms, like the recently proposed loop extrusion model in mammals [43, 44] (see chapter XX of the present book), that enhance the contact frequencies along the genome.

E. A dynamical, out-of-equilibrium and stochastic organization

At the interaction strength compatible with biological data ($E_i = -0.1k_bT$), we analyzed the time evolution of chromosome organization. As in [76], we observed that chromatin folding results from the out-of-equilibrium decondensation of the polymeric chain from its initial compact configuration. Figure6A shows $P_c(s)$, the average contact frequency between two loci separated by a genomic distance s, at different time points. Local scales, like the TAD level, reach a (quasi) steady-state within minutes while it take longer for long-range contacts, ranging from dozen of minutes for Mbp-scale contacts to several hours at the 10 Mbp-scale. These predictions are consistent with

experimental observations made on synchronized cells [17, 79] showing that TADs emerge very early in the cell cycle and that the large-scale A/B compartmentalization is gradually increases along the cell cycle. Even at long time (20 hours or more), the model predicts that the system is not at equilibrium, a regime where we should expect that $P_c(s)$ behaves as $\sim s^{-1.5}$ [77]. On contrary, due to strong topological constraints, the chains remain in a "crumpled", unknotted, confined state with $P_c(s) \sim s^{-1.1}$ for $s < 3$ Mbp (crumpling signature [50, 77, 82]) and $P_c(s) \sim s^{-0.5}$ for $s > 3$Mbp (confinement in chromosome territory [79]), also consistent with Hi-C data [1, 8, 56].

Tracking of the relative distances between pairs of loci revealed that chromatin organization is very stochastic. Figure 6B shows three examples of the time evolution along one cell cycle of such distance for the same pair of loci separated by 3 Mbp along the genome and having the same epigenomic state. We observed a typical two-state behavior with random transitions between a bound state where both loci remain in contacts due to the merging of the TADs they belong to, and a unbound state where both TADs are spatially separated. Analysis of these trajectories for various pairs of loci showed that the transition rate from the unbound to the bound state is a decreasing function of the genomic distance between the two genomic regions, while the transition rate from the bound to the unbound state mainly depends on the respective epigenomic type of each loci, pairs sharing the same type interacting long-lastly. Interestingly, we predicted that a significant proportion ($5 - 15\%$) of long-range contacts (> 1 Mbp) are not established within one cell cycle. This suggests that the genomic distance between regulatory elements, like promoters and enhancers, should not exceed 1 Mbp to ensure that a physical contact between these elements, prerequisite to an activation or repression event for example, would happen at least once during one cell cycle in order to maintain a stable gene expression. It would be interesting to experimentally test such predictions by simultaneously tracking the spatial distance between a promoter and its enhancer and monitoring the current transcriptional activity [83], for various genomic distances between the two elements.

All this suggests that the 3D chromosome organization in higher eukaryotes is out-of-equilibrium, dynamical and stochastic. This emphasizes the necessity (1) to properly account for the time evolution of such organization in quantitative models of chromosomes, especially for higher eukaryotes where chromosomes are strongly topologically constrained; and (2) to well initiate the simulations with proper configurations since the system will keep a partial memory of the large-scale initial structure during a long time window.

F. Relation to other approaches

The prediction of long-range interactions is inherent to copolymer models arranged in blocks. Therefore, such models should also be well adapted to describe the active/inactive compartmentalization in mammals. Several approaches have used similar formalisms to model chromatin folding in human or mouse [61, 84–94]. In particular, the groups of Wolynes and Onuchic [84, 85], of Thirumalai and Hyeon [86, 87], of Mirny [88] or of Liberman-Aiden [61] have developed block copolymer models, eventually decorated with loop extrusion mechanisms or specific-pairwise interactions between CTCF sites at TAD boundaries. Nicodemi's [89–91] and Marenduzzo's [92–94] groups developed more detailed models accounting for the diffusion and binding of the proteins that mediate epigenomic interactions. Most of these approaches lead to very precise descriptions of chromosome organization and of heterochromatin/euchromatin phase separation in mammals. In many cases, their conclusions were very consistent with ours in drosophila: interaction strengths between genomic loci are weak leading to a mild (micro)phase separation and to very dynamical and

stochastic organization.

This idea that the observed phase separation emerges from heterogeneities in the chromatin primary sequence, in analogy to the well-known physical behavior of synthetic block copolymers [74], is quite general and may arise from other possible mechanisms like active non-equilibrium processes or differences in monomer mobilities [95–97]. At a more phenomenological scale, such compartmentalization may be also interpreted as visco-elastic or liquid phase transitions [94, 98, 99] by using an effective phase-field formalism considering euchromatin and heterochromatin as separated fluids and neglecting the underlying polymeric structure.

IV. ROLE OF 3D ORGANIZATION IN EPIGENOME STABILITY

As discussed before, the spatial organization of chromatin results in part from the clustering and phase-segregation of epigenomic domains but a still open question is whether this peculiar 3D folding is only a by-product of genome activity or is also participating to the regulation of the epigenome assembly and more generally to the regulation of the genome functions.

A. The "nano-reactor" hypothesis

The basic concept behind this structural/functional coupling is the augmentation of the local concentration of regulatory proteins due to spatial co-localization. In bacteria, this "high concentration" paradigm has been evidenced and formalized for many years for the well-known lac operon system [100, 101]: molecular crowding and spatial confinement increase the binding affinities of regulators (activators or repressors) to their DNA cognate sequences. This property is enhanced by the presence of few additional dispersed recruitment sequences (operators) and the ability of the lac-repressor to oligomerize, leading to DNA looping. Similarly, in eukaryotes, the nuclear chromatin compartments would correspond to biochemical "nano-reactors" where a few number of regulatory biomolecules are co-localized in space favoring their chemical (co-)activity. At the level of enhancer-promoter genomic modules, the distal action of enhancers is conditioned to their physical proximity with promoters [83]. The presence of different dispersed modules would increase the probability of first contact between the promoter and one enhancer. The subsequent coalescence of the different modules would then provide both structural stability to the ensemble (i.e. increased duration of gene expression) and robustness and precision through the integration of different signals [102]. Along the same line, Polycomb-mediated repression involves the spatial colocalization of silencer sequences (the so-called PREs) of several genes. This is mediated by the Polycomb protein complex that forms multi-loop structures, the so-called polycomb bodies [103–105]. Such clustering operates *in cis*, ie within an epigenomic domain but also *in trans* between non-consecutive domains along the genome. For example, in drosophila, strong long-range interactions are observed between the 10-Mbp distant, Polycomb-marked antennapedia (ANT-C) and bithorax (BX-C) domains [56, 106]. Similarly, in the yeast SIR-mediated heterochromatinisation system, silencing of subtelomeric genes is associated to the level of SIR-mediated clustering [107]. Such clustering might enhance the local concentration of heterochromatin factors (the SIR proteins) at their telomeric specific recruiting sites and consequently might promote their spreading over the subtelomeric domains.

All this suggests that the spatial confinement of regulatory sequences (enhancers, silencers) may allow sequestering

regulatory proteins in the spatial vicinity of the target genomic elements. TADs would correspond to insulated neighborhood that provide a local, basal level of confinement and of selectivity that are then eventually finely-tuned at lower scale (via promoter-enhancer looping for example) [32, 46, 108, 109]. Similarly, formation of A/B compartments would reinforce such properties for TADs sharing similar transcriptional activity or epigenomic state.

B. Epigenomic 1D-3D positive feedback

In the context of epigenomics, the nano-reactor hypothesis introduces naturally a functional coupling between 3D organization and 1D epigenomic states. Indeed, locally, chromatin states are characterized by specific histone marks that favor the selective binding of regulatory proteins (e.g., PcG for H3K27me3, HP-1 of H3K9me3 or transcription factors for active marks) that can self-associate. Hence, the presence of these marks indirectly promotes 3D clustering and compartmentalization via the mechanisms discussed in Sec.III. Moreover, these marks are dynamically deposited and removed by specific enzymatic complexes (e.g., PRC2 or Su(Var)3-0) that physically associate either with the mark they catalyze (eg., H3K27me3 or H3K9me3) or with the corresponding regulatory proteins (e.g, PRC1 or HP1). This "reader-writer/eraser" property enables the mark and thus the chromatin state to spread once nucleated at some specific genomic loci. The crucial point is that spreading might operate not only *in cis*, ie unidimensionnally along the genome, but also *in trans* to any chromatin fragments in the spatial vicinity. This would introduce a positive feedback between the epigenomic state dynamics and the compaction of chromatin: within a given domain the spatial clustering would enhance the "spreading" of the chromatin state over the entire domain (the nano-reactor hypothesis) which in return would enhance compaction (copolymer model).

The ability of enzymes to act *in trans* is clearly a working hypothesis that relies on the assumption that the mechanisms controlling *cis* spreading might also function in *trans*. The molecular processes involved in *trans* (and even in *cis*) spreading of an enzymatic activity to adjacent nucleosomes are still not well understood. Experimental studies on the heterochromatinization in fission yeast have shown that *cis* spreading was not due to allosteric changes of the involved enzymes but more likely to the favorable/stable spatial and orientational arrangement of the enzyme relatively to the histone tails of adjacent nucleosomes [110]. Compact chromatin organization induced by architectural proteins such as HP1 or PRC1 might thus reinforce such *cis* activity [111]. Whether or not such process is restricted to nucleosome *in cis* or can also apply to any spatially proximal nucleosome *in trans*, is unknown. Propagation of silencing in *trans* at the nucleosomal array scale have been evidenced in the Polycomb system [112] but a precise molecular description of this process remains to be elucidated. *In vitro* experiments similar to [110–112] with more extended engineered arrays of nucleosomes will be required for a better understanding of the *cis* vs. *trans* spreading mechanisms. At a more coarse-grained scale, some experiments have also pointed out the possible role of *trans*-acting "long-range" spreading in epigenome maintenance as for heterochromatin domain in yeast [113] or for dosage compensation systems where the propagation of a specific epigenomic signal was associated to the global compaction of sexual chromosomes[109, 114].

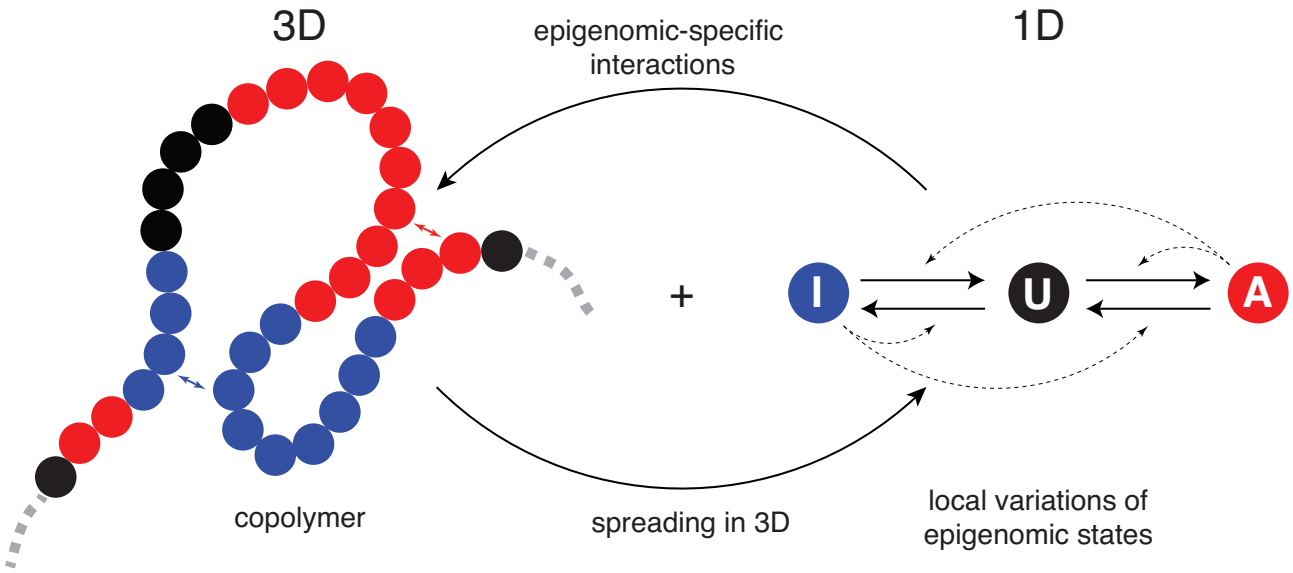

FIG. 7: **The Living chromatin model.** The living chromatin model is a combination of the copolymer model where the chromatin organization is driven by epigenomic-specific contact interactions (Right), and of the epigenome regulation model (Left) where the local epigenomic state of each monomer can fluctuate between 3 states: A, U and I. The inter-conversion (spreading) dynamics between these states depends on the spatial neighborhood of each monomer while the 3D folding depends on the current - primary - epigenomic sequence.

C. The Living Chromatin model

While theoretical and experimental works on the epigenome assembly based on the "reader-writer/eraser" mechanism have highlighted the role of long-range spreading in the stable formation and maintenance of epigenomic domain [113, 115–121], all these approaches neglect the effect of the local chromatin state on the spatial folding of the underlying polymer. To formalize and characterize the 1D-3D positive feedback described above, we developed a theoretical framework, the "Living Chromatin" (LC) model, that explicitly couples the spreading of epigenomic marks to the 3D folding of the fiber (Fig. 7) [72, 122].

This model is a combination of the epigenome regulation model [117, 123] primarily introduced by Dodd *et al.* [115] and the block copolymer model of chromatin [60, 71–73] described in Sec.III. It belongs to the general class of annealed copolymer models where the physico-chemical state of a monomer can vary according to specific reaction rules [124]. The dynamics of the polymer chain follows the block copolymer model described in Sec.III A with short-range contact interactions between monomers having the same state (only for A and I, no interaction between U monomers). For the dynamics of the local epigenomic state, as in [115, 117], we considered a simple case where the state of one monomer can fluctuate only between three flavors: an inactive (I), an active (A) and an intermediate, unmarked (U) state. Conversions between A and I states occur via a first step of mark removal toward the U state followed by a step of mark deposition (Fig. 7 right). Each step can be decomposed into two contributions: (i) a "noisy" conversion accounting for the leaky activity of modifying enzymes or for nucleosome turnover; and (ii) a recruited conversion, formalizing the "reader-writer/eraser" mechanism, where spreading/erasing of a mark is not restricted to neighboring chromatin elements along the genome but also to any fragments located in the *spatial*

neighborhood (Fig. 7 left). To characterize in details the role of 3D organization in this process, we distinguished between *cis* (only via NN monomers along the chain) and *trans* (3D vicinity) conversions. Physically speaking, the LC model is analogous to a 3-state Ising spin system on a polymer chain with local 3D ferromagnetic coupling: the local epigenomic state stands for spin, random conversions for the temperature and recruited conversions for the coupling.

Practically, we modeled the polymer on a lattice following a KMC scheme slightly different from Sec.III B to account for the dynamics of epigenomic states [122]. One MCS consists in (i) N trial monomer state conversions, (ii) $N/2$ trial binding/unbinding transitions; and (iii) N trial monomer moves. In (i) a monomer m is randomly picked and a state transition is attempted according to the state-dependent rates:

$$k_{A\to U}(m) = k_{U\to I}(m) \;=\; \epsilon_o + \epsilon_c \left(\Theta_{e(m-1),I} + \Theta_{e(m+1),I}\right) + \epsilon_t \sum_{l\neq(m-1:m+1)} \Theta_{e(l),I}\delta_{l,m} \tag{2}$$

$$k_{I\to U}(m) = k_{U\to A}(m) \;=\; \epsilon_o + \epsilon_c \left(\Theta_{e(m-1),A} + \Theta_{e(m+1),A}\right) + \epsilon_t \sum_{l\neq(m-1:m+1)} \Theta_{e(l),A}\delta_{l,m} \tag{3}$$

with $e(l) \in \{A, U, I\}$ the current epigenomic state of monomer l, ϵ_o the contribution of noisy conversion, ϵ_c (resp. ϵ_t) the spreading rate *in cis* (resp. *in trans*), $\Theta_{e(l),X} = 1$ if $e(l) = X$ (0 otherwise) and $\delta_{l,m} = 1$ if monomers l and m occupy NN sites on the lattice (0 otherwise). For simplicity, we assumed that the rates ϵ_o, ϵ_c and ϵ_t are the same for all the states. In (ii) a monomer m is randomly picked and if its state is either A or I, for every monomer l of the same state occupying a NN site on the lattice and already bound to m, an unbinding event is attempted with a rate k_u. Similarly for unbound pairs, a binding event is realized with a rate k_b. In (iii), a monomer is randomly picked and move to a NN site on the lattice. The move is accepted only if the connexions along the chain and between the bound monomers are maintained. To simplify, we focused our studies on small chains at steady-state, neglecting crumpling effects described in Sec.III.

D. Stability of one epigenomic domain

In a recent study [122], we investigated the behavior of an isolated small chain ($N = 100$) evolving under the LC model as a function of the attraction strength k_b/k_u and of the relative conversion rates $\epsilon_{c,t}/\epsilon_o$. Here, we report a similar analysis but for a longer chain ($N \approx 200$) in a semi-dilute environment (10% volumic density), simulated using periodic boundary condition [60]. Following the analogy with an Ising model, we characterized the global epigenomic state S of the system using an effective magnetization:

$$S = \frac{1}{N}\sum_{l=1}^{N}\left(\Theta_{e(l),A} - \Theta_{e(l),I}\right) \tag{4}$$

$S \sim +1$ (resp. -1) implies that the full domain is in a coherent A (resp. I) macro-state where most of the monomers have a A (resp. I) state. $S \sim 0$ defines a globally incoherent epigenomic state with a mixture of A, U and I monomers.

In absence of *trans* spreading ($\epsilon_t = 0$), the LC model reduces to a simple system where the epigenomic dynamics is disconnected to the 3D polymeric organization and evolves only under short-range 1D spreading. As expected for 1D system driven only by NN processes, no phase transition is observed in this case and the distribution of S remains peaked around 0. The existence of stable coherent active (A) or inactive (I) macrostates is unlikely (Fig. 8I).

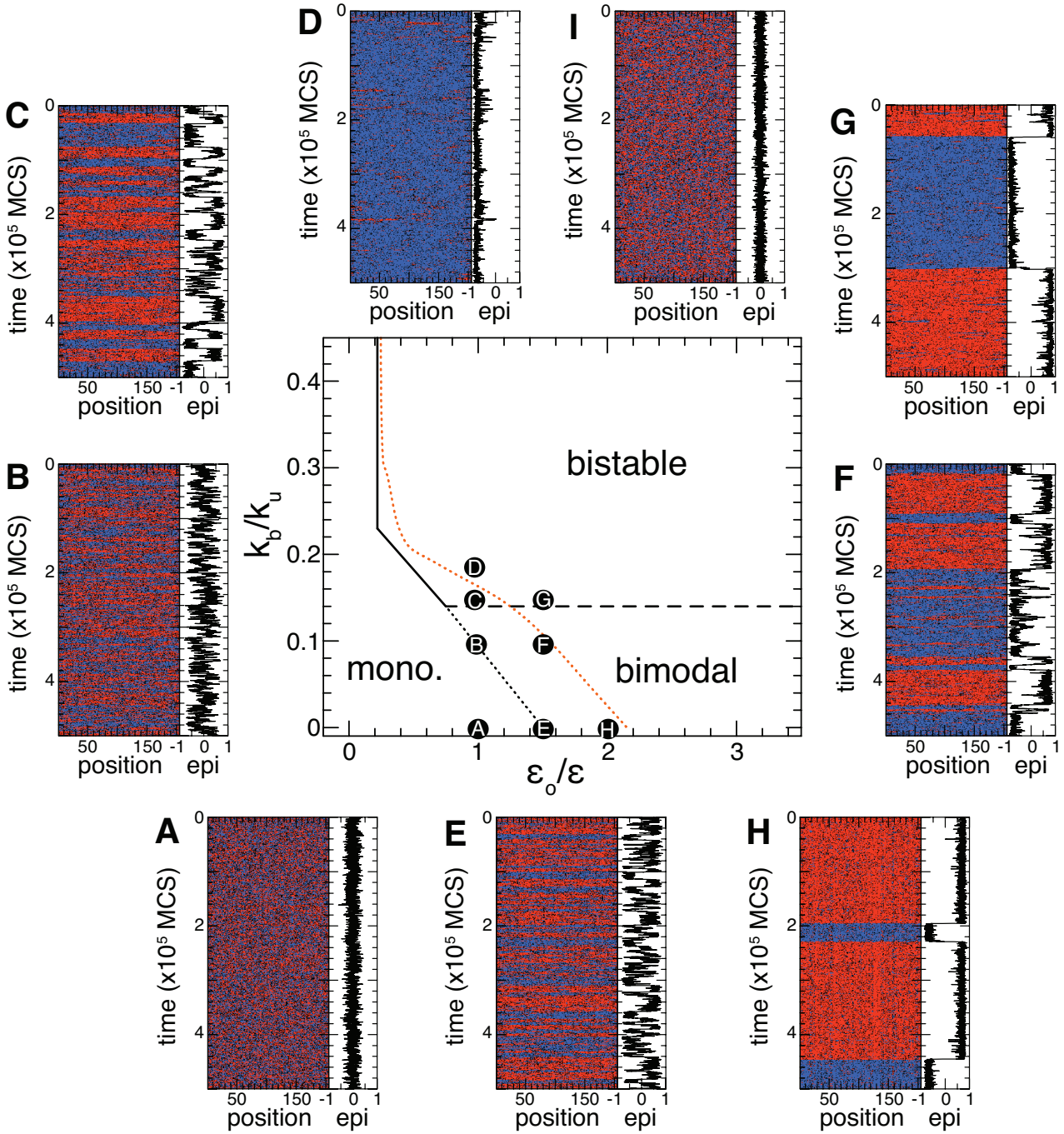

FIG. 8: **Phase diagram of one epigenomic domain** ($\epsilon_c = \epsilon_t \equiv \epsilon$, $\epsilon_o = 0.001$, $k_u = 0.001$). The monostable, bistable and bimodal regions are demarcated by black lines. The corresponding curves for an isolated shorter chain as investigated in [122] is reported for comparison (orange lines). (A-H) Examples of time evolution of the local epigenomic state (Left: red for A, blue for I and black for U) and of the global epigenomic state S (Right), for various values of ϵ/ϵ_o and k_b/k_u (noted as black dots in the phase diagram) predicted by the full LC model.(I) Same as (A-H) but when *trans* spreading was neglected ($\epsilon_c = 0.2,\ \epsilon_t = 0$).

In presence of *trans* spreading, this simple picture is dramatically modified. In Fig.8, we plotted the phase diagram of the system as a function of k_b/k_u and ϵ/ϵ_o where we assumed that $\epsilon_c = \epsilon_t \equiv \epsilon$. At weak attraction strength ($k_b/k_u \lesssim 0.1$), the polymer has a swollen organization. While for $\epsilon/\epsilon_o \lesssim 1-1.5$ the system remains monostable with a globally incoherent epigenome characterized by short-lived coexisting A and I microdomains (Fig. 8A, B, E), at high ϵ the weak *trans* spreading activity due to the presence of (some) random long-range contacts allows the emergence of coherent epigenomic domains (Fig. 8H,F). Strictly speaking, this transition from monostability (incoherent state) to bimodality (coherent A and I macrostates) does not reflect a phase transition but rather is a signature of finite size effects. Hence, the stability of a macrostate increases linearly with ϵ [122].

As k_b/k_u augments, the polymeric system exhibits a collapse transition where the chain passes from a swollen coil to a compact globule [125]. Above this collapse, for ϵ higher than a critical, k_b/k_u-dependent recruitment strength, we observed a second-order phase transition towards a bistable regime (Fig.8C,D,G). In this phase, cooperative effects are dominant and lead to the emergence of super-stable A or I macro-states (stability increases exponentially with ϵ [122]). This is characteristics of the presence of phase transitions in 1D systems with effective long-range interactions only if the strength of interactions between two monomers l and m decreases more slowly than $1/|m-l|^2$ [126], *i.e.*, in our case, only if epigenomic-driven interactions (via k_b/k_u) are strong enough to partially collapse the polymer so that the contact probability between two monomers scales slower than $1/|m-l|^2$.

As already shown in [115, 117], these results confirmed that the emergence and maintenance of stable coherent macro-states require an efficient *trans* spreading activity. Moreover, accounting explicitly for the polymeric structure and for the impact of epigenomic-driven interactions suggested that physical bridging may strongly enhance the stability of coherent epigenomic domains by creating more compact 3D neighborhood facilitating *trans*-mediated recruited conversions. Comparison with the phase diagram of an isolated chain (orange lines in Fig.8) underlines this effect since accounting for an effective confinement of the chain (via the control of the volumic fraction) reduced the critical value to switch from the monostable, incoherent regime to the bistable/bimodal, coherent one.

E. Stability of antagonistic epigenomic domains

In the previous section, we discussed how *trans* activity coupled to epigenomic-driven interactions affect the stability of a single epigenomic domain. The next step is to understand how such mechanisms impact the epigenomic stability of a genomic region containing several adjacent antagonistic chromatin states (A and I). As a proof of concept, for parameters leading to bistability, we addressed this issue by following the dynamics of a region initially prepared with one (reported in [122]) or two (reported here in Fig 9) I domains directly adjacent to one or two A domains of the same size. In Fig.9A-C, we presented some examples for a region initialized with 4 adjacent epigenomic domains (2 active A, 2 inactive I) forming two distinct 3D compartments (one for A, one for I). In particular, for various situations, we quantified the stability of the 1D epigenomic organization (Fig.9E) by measuring the time it takes for the system to switch from this mosaic initial state to a typical steady-state (coherent A or I macro-states or incoherent state depending on the parameters).

In absence of *trans* spreading activity, each subdomain is very unstable (red dots in Fig.9E) and rapidly converges to a incoherent epigenomic organization. Similarly, accounting for *trans* spreading but neglecting the epigenomic-driven interactions leads to a rapid destabilization of the system (blue dots in Fig.9E) towards a coherent macrostate. It

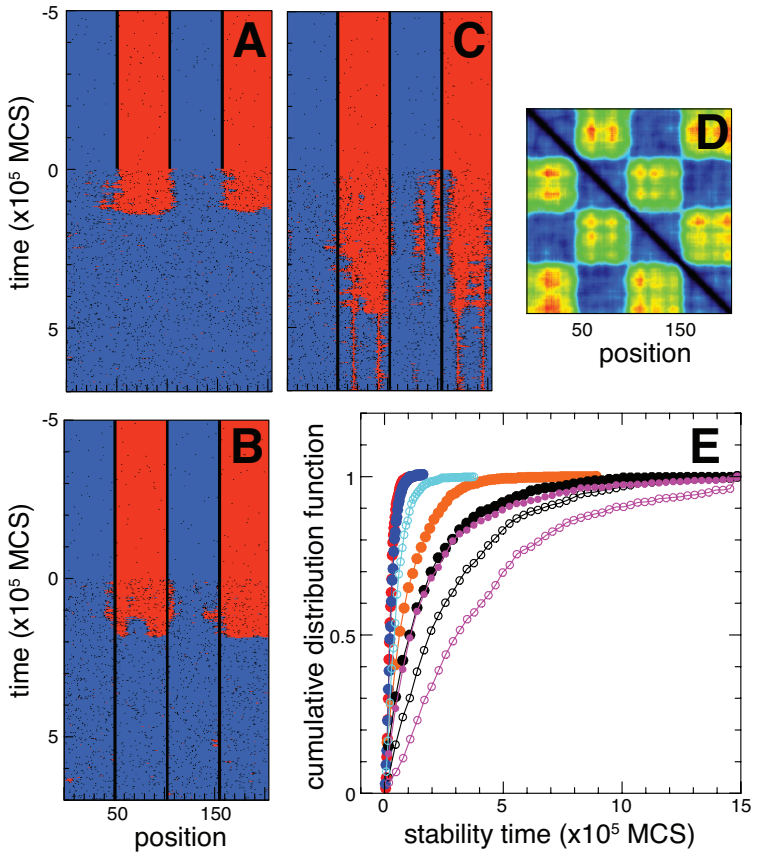

FIG. 9: **Stability of epigenome compartmentalization** ($k_b/k_u = 0.28$,$\epsilon_c = 0.01, \epsilon_t = \epsilon_o = 0.001$). (A-C) Examples of time evolution of the local epigenomic state of genomic region initialized with 4 adjacent epigenomic domains forming two spatial compartments (Average distance map between any pair of monomers shown in (D)) . Initially the state of each subdomain is forced. At $t > 0$ forcing is switched off (except in C where a weak loading rate of 0.001 is maintained). (E) Cumulative distribution of the stability time τ of the mosaic epigenomic pattern with only *cis* recruitment (red dots), without epigenomic-driven interactions (blue dots), with weaker interactions ($k_b/k_u = 0.18$, cyan dots), in absence (orange dots) or presence (purple dots) of 1D barriers, in presence of 1D barriers and weak nucleation (purple circles). Black dots and circles correspond to a system with only 2 epigenomic domains, each of size 50 [122].

is only by fully considering the positive feedback between epigenome and polymer dynamics that the 4 sub-domains remain significantly stable (Fig.9A), the stronger the interactions the more stable the partition (cyan and orange dots in Fig.9E). Indeed, the formation of two distinct, compact spatial compartments for A and I domains limits the "invasion" in *trans* of one epigenomic domain by the antagonistic state of its neighboring domains. This also leads to strong cooperativity between the subdomains of the same epigenomic state that switch their states always at the same time.

A way to enhance the stability of subdomains is to introduce 1D barriers (Fig.9B). By maintaining the monomers at the boundary between two antagonistic subdomains in a neutral U state, we hinder the propagation in *cis* between NN subdomains. Such barriers are biologically-relevant with the binding of insulator proteins such as CTCF at TAD boundaries [46] that can physically prevent the action in *cis* of epigenomic enzymes. External "contamination" of one domain by the other can thus only arises from the *trans* spreading activity across the frontier. This leads to a

significant stabilization by 2 to 3 fold (purple dots in Fig.9E) depending on the size of the barrier [122].

Previously, adjacent antagonistic subdomains were forced to be in one epigenomic state and, at $t > 0$, the system was evolving in absence of forcing. Here, we asked, in association with 1D barriers, how maintaining a weak permanent forcing of the initial state inside each subdomain influence their stability (Fig.9C). This situation mimics the presence of nucleation sites like PREs for H3K27me3/PcG domains. We observed a strong increase of the mean stability time even at low loading rates (purple circles in Fig. 9E). This is fully consistent with recent experimental studies showing that long-term memory relies on self-propagation (in our case promoted by spatial condensation) and on sequence-specific *cis*-recruitment mechanisms [127–129]. Our results suggest that spatial compaction, by promoting self-propagation in *trans*, might cooperate with *cis*-recruitment to achieve strong stability. This means that a weakening of the recruitment might be compensated by an increase of the compaction. Whether this compensatory mechanisms indeed occur in real systems at both developmental and evolutionary time scales [130] has to be further investigated. Interestingly, compared to the case of a chain with only two adjacent subdomains as studied in [122] (black dots and circles in Fig. 9E), we observed that stability is enhanced when considering four adjacent domains. This implies that forming large-scale spatial compartment, like the A/B or heterochromatin/euchromatin compartments, increases the insulation of both antagonistic marks and delays the cooperative switching of subdomains towards a global coherent macro-state.

F. Towards a quantitative model

The LC model represents a powerful theoretical and numerical formalism to study the dynamical coupling between the 1D epigenomic information along the chain and the 3D chromatin organization: 3D acts on 1D via the *trans* spreading mechanism while the 1D feedbacks the 3D via epigenomically-driven contact interactions. This framework is modular and can be easily generalized to any number of epigenomic states and any biochemical reactions or interaction scheme. We showed that an efficient epigenome stability and compartmentalization requires (i) *trans* spreading mechanisms; (ii) eventually 1D barriers and weak permanent nucleation; and (iii) the chain to be collapsed (ie around or below the collapse transition). This latter regime is exactly the condition consistent with experimental Hi-C data as we showed in our previous works on chromatin folding for a fixed epigenome (see Sec.III). However to be applied to *specific in vivo* situations, the LC model should be extended to consider other biologically-relevant ingredients such as titration effects [118, 120], replication and cell cycle duration [115, 123], conversion asymmetries [117] or multicolor epigenome [131]. In order to progress toward a quantitative description of this 1D-3D coupling, a correct parameter inference would require to design experiments that can record the large-scale dynamics of both the 1D and 3D organization, during the establishment and the maintenance stages, in both wild-type and mutant backgrounds. Corresponding experimental techniques remain to be developed.

Recently, Michieletto *et al.* have also developed a physical model of such 1D-3D coupling of chromatin [132]. In their approach, the dynamics of the epigenome and of the polymer are governed by an identical Hamiltonian, ie the spreading of a mark is tightly related to the (pre)existence of chemical bonds with the nearest monomers. This is a main difference with the LC model where spreading *in trans* is not directly coupled to the copolymer dynamics but rather depends only on the presence of monomers in spatial neighborhood. Compared to their approach, the LC framework is somehow more general since we explicitly treat the local epigenomic dynamics as biochemical reactions and not as a Hamiltonian dynamics. In addition, we decomposed the spreading into two contributions (*cis* and *trans*),

that, we think, is crucial to understand clearly the 1D/3D coupling. Our proposed mechanism leads to second-order phase transition while Michieletto *et al.* found first-order transition within their framework. There is, to date, no experimental evidence for one or the other type of transition. More importantly, the main and similar outcome of these two complementary and pioneering studies is that self-attraction and *trans*-spreading activity at the local scale can be translated into a macroscopic coupling between epigenome and spatial compartmentalization dynamics. As shown in [122], the correlated evolution of the global epigenomic state and of the radius of gyration of the chain at the collapse transition illustrates nicely how the local 1D-3D feedback mechanism induces a large scale coupling between the epigenome and the spatial chain folding: incoherent epigenomic states tend to be associated with a partial decondensation of the chain while coherent states correspond to more condensed configurations.

V. DISCUSSION AND PERSPECTIVES

In this chapter, we discussed how polymer modeling allows to better understand the coupling between epigenome and 3D chromosome organization.

In a first part, we showed that epigenomically-associated mechanisms are main drivers of chromosome folding: A/B or heterochromatin/euchromatin compartments in drosophila emerge naturally from the mild microphase separation of different chromatin states that leads to a very dynamical and stochastic organization. Our model predicts that active chromatin only weakly interacts with itself. This may reflect a distinct local mode of interaction between chromatin types: active chromatin rather organizes locally via pairwise short-range bridging between discrete specific genomic sites while heterochromatin may interact more continuously via clustering of multiple chromatin loci. This is consistent with more homogeneous internal contact patterns observed for inactive domains and more complex profiles of contact for active domains as observed in human cell lines [67]. Overall, a finer understanding of these different modes of self-association will require a proper inference of the chromatin-state-specific interaction strength. Thanks to higher-resolution Hi-C and epigenomic data, we expect to gain deeper insights into the complexity of the local epigenomic and genomic control of chromatin self-association. Additionally, interactions with nuclear landmarks such as membrane and nuclear pores are known to play a fundamental role in controlling large-scale nuclear organization [114, 133]. Integration of such interactions in our framework would also lead to a more detailed description of chromatin folding.

In a second part, we addressed the role of 3D organization into epigenomic stability and maintenance. Our working hypothesis is that spatial compartmentalization may provide a favorable environment playing a functional role of "nano-reactor" by confining the proper regulators close to the target regions. TADs might have a role in either preventing (by sequestering) or facilitating the long-range communication between distal regulatory genomic elements, thus enhancing the efficiency of gene co-activation or co-repression [134, 135]. In our copolymer framework, we remarked that experimental observations are compatible with a region of the phase diagram that is sensitive to variations in the interaction strength and in the block size. One could hypothesize that by modulating the number of bridging molecules (or their bridging efficiency), cells might finely tune the local condensation and the long-range contacts between epigenomic domains, and thus might regulate gene expression or epigenomics. To test this, we developed an extended copolymer model, the Living Chromatin model that readily couples the local transition between different chromatin states with the spatial organization of the chain. We demonstrated that epigenome plasticity and robustness is ensured when the chain is in a sufficiently collapsed state which is exactly the physiological

condition. Building on the classical Waddington picture of epigenomic landscape [136], progression through successive developmental or differentiation stages as well as pathologies may now correspond to different pathways on the folding-epigenome landscape with enzymatic activity and self-affinity of architectural chromatin-binding proteins as control parameters.

The ultimate goal would be to build a quantitative model that could reproduce both the complex linear epigenomic pattern and the spatial chromatin organization in real systems such as in drosophila and make testable predictions. However a proper inference of the corresponding parameters would require to account properly for dynamics. Indeed, as discussed above, chromosome folding is out-of-equilibrium, dynamical and stochastic. At the TAD scale (the relevant regulatory scale), the chain reaches rapidly a stationary states. However at larger scales, converge towards a metastable state may be slow. Cell cycle duration then may constitute an additional control parameter: establishment of stable long-range contact might be challenged by cell cycle duration. Efforts toward the development of time-predictive models of the spatial and epigenomic organization are required. We already managed to calibrate the copolymer model from MSD measurement of chromatin loci such that we can have a reliable description of chromosome folding kinetics. However we still lack a precise time-parameterization of the local epigenome dynamics. Furthermore, we do not consider the out-off equilibrium effect of replication which is of course a really important issue to understand epigenetic maintenance. Incorporating all these ingredients into a quantitative, predictive model would represent an intriguing challenging task for the future on both theoretical and experimental sides.

Acknowledgements

We apologize to colleagues which work could not be cited due to space constraints. We thank Guido Tiana and Luca Giorgetti for inviting us to write this chapter. We are grateful to Surya Ghosh, Angelo Rosa, Ralf Everaers, Pascal Carrivain, Ivan Junier, Peter Meister and Giacomo Cavalli for fruitful discussions. We acknowledge our funding agencies: Agence Nationale de la Recherche (ANR-15-CE12-0006 EpiDevoMath), Fondation pour la Recherche Médicale (DEI20151234396) and CNRS. Computing resources were provided by the CIMENT infrastructure at University Grenoble-Alpes (supported by the Rhône-Alpes region, Grant CPER07 13 CIRA) and by the Pôle Scientifique de Modélisation Numérique and Centre Blaise Pascal at ENS Lyon.

---

[1] Rao, S. S. P., Huntley, M. H., Durand, N. C., Stamenova, E. K., Bochkov, I. D., Robinson, J. T., Sanborn, A. L., Machol, I., Omer, A. D., Lander, E. S., and Aiden, E. L. A 3d map of the human genome at kilobase resolution reveals principles of chromatin looping. *Cell* **159**(7), 1665–80, Dec (2014).

[2] Durand, N. C., Robinson, J. T., Shamim, M. S., Machol, I., Mesirov, J. P., Lander, E. S., and Lieberman Aiden, E. Juicebox provides a visualization system for hi-c contact maps with unlimited zoom. *Cell Systems* **3**, 99–101 (2016).

[3] de Wit, E. and de Laat, W. A decade of 3c technologies: insights into nuclear organization. *Genes Dev* **26**, 11–24 (2012).

[4] Cremer, C., Szczurek, A., Schock, F., Gourram, A., and Birk, U. Super-resolution microscopy approaches to nuclear nanostructure imaging. *Methods* **123**, 11–32 (2017).

[5] Dixon, J. R., Selvaraj, S., Yue, F., Kim, A., Li, Y., Shen, Y., Hu, M., Liu, J. S., and Ren, B. Topological domains in mammalian genomes identified by analysis of chromatin interactions. *Nature* **485**(7398), 376–380, May (2012).

[6] Nora, E. P., Lajoie, B. R., Schulz, E. G., Giorgetti, L., Okamoto, I., Servant, N., Piolot, T., van Berkum, N. L., Meisig, J., Sedat, J., Gribnau, J., Barillot, E., Blüthgen, N., Dekker, J., and Heard, E. Spatial partitioning of the regulatory landscape of the x-inactivation centre. *Nature* **485**(7398), 381–385, May (2012).

[7] Boettiger, A. N., Bintu, B., Moffitt, J. R., Wang, S., Beliveau, B. J., Fudenberg, G., Imakaev, M., Mirny, L. A., Wu, C.-t., and Zhuang, X. Super-resolution imaging reveals distinct chromatin folding for different epigenetic states. *Nature* **529**(7586), 418–422, Jan (2016).

[8] Lieberman-Aiden, E., van Berkum, N. L., Williams, L., Imakaev, M., Ragoczy, T., Telling, A., Amit, I., Lajoie, B. R., Sabo, P. J., Dorschner, M. O., Sandstrom, R., Bernstein, B., Bender, M. A., Groudine, M., Gnirke, A., Stamatoyannopoulos, J., Mirny, L. A., Lander, E. S., and Dekker, J. Comprehensive mapping of long-range interactions reveals folding principles of the human genome. *Science* **326**(5950), 289–293, Oct (2009).

[9] Cremer, T., Cremer, M., Hbner, B., Strickfaden, H., Smeets, D., Popken, J., Sterr, M., Markaki, Y., Rippe, K., and Cremer, C. The 4d nucleome: Evidence for a dynamic nuclear landscape based on co-aligned active and inactive nuclear compartments. *FEBS Letters* **589**, 2931–2943 (2015).

[10] Biggiogera, M., Courtens, J.-L., Derenzini, M., Fakan, S., Hernandez-Verdun, D., Risueno, M.-C., and Soyer-Gobillard, M.-O. Osmium ammine: Review of current applications to visualize dna in electron microscopy. *Biol. Cell* **87**, 121–132 (1996).

[11] Mattout, A., Cabianca, D. S., and Gasser, S. M. Chromatin states and nuclear organization in development - a view from the nuclear lamina. *Genome Biology* **16**, 174 (2015).

[12] Towbin, B. D., Meister, P., and Gasser, S. M. The nuclear envelopea scaffold for silencing? *Current Opinion in Genetics & Development* **19**(2), 180 – 186 (2009).

[13] Meuleman, W., Peric-Hupkes, D., Kind, J., Beaudry, J.-B., Pagie, L., Kellis, M., Reinders, M., Wessels, L., and van Steensel, B. Constitutive nuclear lamina-genome interactions are highly conserved and associated with a/t-rich sequence. *Genome Research* **23**, 270–280 (2013).

[14] Bolzer, A., Kreth, G., Solovei, I., Koehler, D., Saracoglu, K., Fauth, C., Muller, S., Eils, R., Cremer, C., Speicher, M. R., and Cremer, T. Three-dimensional maps of all chromosomes in human male fibroblast nuclei and prometaphase rosettes. *PLoS Biology* **3**, e157 (2005).

[15] Gerlich, D., Beaudouin, J., Kalbfuss, B., Daigle, N., Eils, R., and Ellenberg, J. Global chromosome positions are transmitted through mitosis in mammalian cells. *Cell* **112**(6), 751 – 764 (2003).

[16] Nagano, T., Lubling, Y., Stevens, T. J., Schoenfelder, S., Yaffe, E., Dean, W., Laue, E. D., Tanay, A., and Fraser, P. Single-cell hi-c reveals cell-to-cell variability in chromosome structure. *Nature* **502**(7469), 59–64, Oct (2013).

[17] Nagano, T., Lubling, Y., Varnai, C., Dudley, C., Leung, W., Baran, Y., Cohen, N. M., Wingett, S., Fraser, P., and Tanay, A. Cell cycle dynamics of chromosomal organisation at single-cell resolution. *bioRxiv* **10.1101**, 094466 (2016).

[18] Stevens, T. J., Lando, D., Basu, S., Atkinson, L. P., Cao, Y., Lee, S. F., Leeb, M., Wohlfahrt, K. J., Boucher, W., OShaughnessy-Kirwan, A., et al. 3d structures of individual mammalian genomes studied by single-cell hi-c. *Nature* **544**, 59–64 (2017).

[19] Flyamer, I. M., Gassler, J., Imakaev, M., Brandao, H. B., Ulianov, S. V., Abdennur, N., Razin, S. V., Mirny, L. A., and Tachibana-Konwalski, K. Single-nucleus hi-c reveals unique chromatin reorganization at oocyte-to-zygote transition. *Nature* **544**, 110–114 (2017).

[20] Wang, S., Su, J.-H., Beliveau, B. J., Bintu, B., Moffitt, J. R., Wu, C.-t., and Zhuang, X. Spatial organization of chromatin domains and compartments in single chromosomes. *Science* **353**, 598–602 (2016).

[21] Cattoni, D. I., Gizzi, A. M. C., Georgieva, M., Di Stefano, M., Valeri, A., Chamousset, D., Houbron, C., Dejardin, S., Fiche, J.-B., Gonzalez, I., Chang, J.-M., Sexton, T., Marti-Renom, M. A., Bantignies, F., Cavalli, G., and Nollmann, M. Single-cell absolute contact probability detection reveals chromosomes are organized by multiple low-frequency yet

specific interactions. *Nature Communications* **8**, 1753 (2017).

[22] Bystricky, K. Chromosome dynamics and folding in eukaryotes: Insights from live cell microscopy. *FEBS Letters* **589**, 3014–3022 (2015).

[23] Hajjoul, H., Mathon, J., Ranchon, H., Goiffon, I., Mozziconacci, J., Albert, B., Carrivain, P., Victor, J.-M., Gadal, O., Bystricky, K., and Bancaud, A. High-throughput chromatin motion tracking in living yeast reveals the flexibility of the fiber throughout the genome. *Genome Res* **23**(11), 1829–1838, Nov (2013).

[24] Germier, T., Kocanova, S., Walther, N., Bancaud, A., Shaban, H. A., Sellou, H., Politi, A. Z., Ellenberg, J., Gallardo, F., and Bystricky, K. Real-time imaging of a single gene reveals transcription-initiated local confinement. *Biophysical Journal* **113**, 1383–1394 (2017).

[25] Bronstein, I., Israel, Y., Kepten, E., Mai, S., Shav-Tal, Y., Barkai, E., and Garini, Y. Transient anomalous diffusion of telomeres in the nucleus of mammalian cells. *Phys Rev Lett* **103**(1), 018102, Jul (2009).

[26] Shinkai, S., Nozaki, T., Maeshima, K., and Togashi, Y. Dynamic nucleosome movement provides structural information of topological chromatin domains in living human cells. *PLOS Computational Biology* **12**(10), 1–16, 10 (2016).

[27] Nozaki, T., Imai, R., Tanbo, M., Nagashima, R., Tamura, S., Tani, T., Joti, Y., Tomita, M., Hibino, K., Kanemaki, M. T., Wendt, K. S., Okada, Y., Nagai, T., and Maeshima, K. Dynamic organization of chromatin domains revealed by super-resolution live-cell imaging. *Molecular Cell* **67**, 282–293 (2017).

[28] Lucas, J. S., Zhang, Y., Dudko, O. K., and Murre, C. 3d trajectories adopted by coding and regulatory dna elements: First-passage times for genomic interactions. *Cell* **158**, 339352 (2014).

[29] Ruiz-Velasco, M. and Zaugg, J. B. Structure meets function: how chromatin organisation conveys functionality. *Current Opinion in Systems Biology* **1**, 129–136 (2017).

[30] Kaiser, V. B. and Semple, C. A. When tads go bad: chromatin structure and nuclear organisation in human disease. *F1000Research* **6** (2017).

[31] Corces, M. R. and Corces, V. G. The three-dimensional cancer genome. *Current opinion in genetics & development* **36**, 1–7 (2016).

[32] Zhan, Y., Mariani, L., Barozzi, I., Schulz, E., Bluthgen, N., Stadler, M., Tiana, G., and Giorgetti, L. Reciprocal insulation analysis of hi-c data shows that tads represent a functionally but not structurally privileged scale in the hierarchical folding of chromosomes. *Genome Research* **27**, 479–490 (2017).

[33] Quintero-Cadena, P. and Sternberg, P. W. Enhancer sharing promotes neighborhoods of transcriptional regulation across eukaryotes. *G3: Genes, Genomes, Genetics* **6**, 4167–4174 (2016).

[34] Hnisz, D., Weintraub, A. S., Day, D. S., Valton, A.-L., Bak, R. O., Li, C. H., Goldmann, J., Lajoie, B. R., Fan, Z. P., Sigova, A. A., Reddy, J., Borges-Rivera, D., Ihn Lee, T., Jaenisch, R., Porteus, M. H., Dekker, J., and Young, R. A. Activation of proto-oncogenes by disruption of chromosome neighborhoods. *Science* **351**, 14541458 (2016).

[35] Lupiáñez, D. G., Kraft, K., Heinrich, V., Krawitz, P., Brancati, F., Klopocki, E., Horn, D., Kayserili, H., Opitz, J. M., Laxova, R., Santos-Simarro, F., Gilbert-Dussardier, B., Wittler, L., Borschiwer, M., Haas, S. A., Osterwalder, M., Franke, M., Timmermann, B., Hecht, J., Spielmann, M., Visel, A., and Mundlos, S. Disruptions of topological chromatin domains cause pathogenic rewiring of gene-enhancer interactions. *Cell* **161**(5), 1012–1025, May (2015).

[36] Jost, D., Vaillant, C., and Meister, P. Coupling 1d modifications and 3d nuclear organization: data, models and function. *Curr Opin Cell Biol* **44**, 20–27 (2017).

[37] Pombo, A. and Dillon, N. Three-dimensional genome architecture: players and mechanisms. *Nature reviews Molecular cell biology* **16**, 245–257 (2015).

[38] Canzio, D., Liao, M., Naber, N., Pate, E., Larson, A., Wu, S., Marina, D. B., Garcia, J. F., Madhani, H. D., Cooke, R., Schuck, P., Cheng, Y., and Narlikar, G. J. A conformational switch in hp1 releases auto-inhibition to drive heterochromatin assembly. *Nature* **496**(7445), 377–381, Apr (2013).

[39] Isono, K., Endo, T. A., Ku, M., Yamada, D., Suzuki, R., Sharif, J., Ishikura, T., Toyoda, T., Bernstein, B. E., and Koseki, H. Sam domain polymerization links subnuclear clustering of prc1 to gene silencing. *Dev Cell* **26**(6), 565–577, Sep (2013).

[40] Larson, A. G., Elnatan, D., Keenen, M. M., Trnka, M. J., Johnston, J. B., Burlingame, A. L., Agard, D. A., Redding, S., and Narlikar, G. J. Liquid droplet formation by hp1α suggests a role for phase separation in heterochromatin. *Nature* **547**, 236–240 (2017).

[41] Strom, A. R., Emelyanov, A. V., Mir, M., Fyodorov, D. V., Darzacq, X., and Karpen, G. H. Phase separation drives heterochromatin domain formation. *Nature* **547**, 241–245 (2017).

[42] Ulianov, S., Shevelyov, Y., and Razin, S. Lamina-associated chromatin in the context of the mammalian genome folding. *Biopolymers and Cell* **32**, 327–333 (2016).

[43] Sanborn, A. L., Rao, S. S. P., Huang, S.-C., Durand, N. C., Huntley, M. H., Jewett, A. I., Bochkov, I. D., Chinnappan, D., Cutkosky, A., Li, J., Geeting, K. P., Gnirke, A., Melnikov, A., McKenna, D., Stamenova, E. K., Lander, E. S., and Aiden, E. L. Chromatin extrusion explains key features of loop and domain formation in wild-type and engineered genomes. *Proc Natl Acad Sci U S A* **112**(47), E6456–E6465, Nov (2015).

[44] Fudenberg, G., Imakaev, M., Lu, C., Goloborodko, A., Abdennur, N., and Mirny, L. A. Formation of chromosomal domains by loop extrusion. *Cell Rep* **15**(9), 2038–2049, May (2016).

[45] Dekker, J. and Mirny, L. The 3d genome as moderator of chromosomal communication. *Cell* **164**, 1110–1121 (2016).

[46] Dowen, J. M., Fan, Z. P., Hnisz, D., Ren, G., Abraham, B. J., Zhang, L. N., Weintraub, A. S., andTong Ihn Lee, J. S., and Zhao, K. Control of cell identity genes occurs in insulated neighborhoods in mammalian chromosomes. *Cell* **159**, 374–387 (2014).

[47] Amitai, A. and Holcman, D. Polymer physics of nuclear organization and function. *Physics Reports* **678**, 1–83 (2017).

[48] Cortini, R., Barbi, M., Car, B., Lavelle, C., Lesne, A., Mozziconacci, J., and Victor, J.-M. The physics of epigenetics. *Rev Mod Phys* **88**, 025002 (2016).

[49] Rosa, A. and Zimmer, C. Computational models of large-scale genome architecture. *Int Rev Cell Mol Biol* **307**, 275–349 (2014).

[50] Halverson, J. D., Smrek, J., Kremer, K., and Grosberg, A. Y. From a melt of rings to chromosome territories: the role of topological constraints in genome folding. *Rep Prog Phys* **77**(2), 022601 (2014).

[51] Ho, J. W. K., Jung, Y. L., Liu, T., Alver, B. H., Lee, S., Ikegami, K., Sohn, K.-A., Minoda, A., Tolstorukov, M. Y., Appert, A., Parker, S. C. J., Gu, T., Kundaje, A., Riddle, N. C., Bishop, E., Egelhofer, T. A., Hu, S. S., Alekseyenko, A. A., Rechtsteiner, A., Asker, D., Belsky, J. A., Bowman, S. K., Chen, Q. B., Chen, R. A.-J., Day, D. S., Dong, Y., Dose, A. C., Duan, X., Epstein, C. B., Ercan, S., Feingold, E. A., Ferrari, F., Garrigues, J. M., Gehlenborg, N., Good, P. J., Haseley, P., He, D., Herrmann, M., Hoffman, M. M., Jeffers, T. E., Kharchenko, P. V., Kolasinska-Zwierz, P., Kotwaliwale, C. V., Kumar, N., Langley, S. A., Larschan, E. N., Latorre, I., Libbrecht, M. W., Lin, X., Park, R., Pazin, M. J., Pham, H. N., Plachetka, A., Qin, B., Schwartz, Y. B., Shoresh, N., Stempor, P., Vielle, A., Wang, C., Whittle, C. M., Xue, H., Kingston, R. E., Kim, J. H., Bernstein, B. E., Dernburg, A. F., Pirrotta, V., Kuroda, M. I., Noble, W. S., Tullius, T. D., Kellis, M., MacAlpine, D. M., Strome, S., Elgin, S. C. R., Liu, X. S., Lieb, J. D., Ahringer, J., Karpen, G. H., and Park, P. J. Comparative analysis of metazoan chromatin organization. *Nature* **512**(7515), 449–52, Aug (2014).

[52] Filion, G. J., van Bemmel, J. G., Braunschweig, U., Talhout, W., Kind, J., Ward, L. D., Brugman, W., de Castro, I. J., Kerkhoven, R. M., Bussemaker, H. J., et al. Systematic protein location mapping reveals five principal chromatin types in drosophila cells. *Cell* **143**(2), 212–224 (2010).

[53] Roudier, F. and other. Integrative epigenomic mapping defines four main chromatin states in arabidopsis. *EMBO J* **30**(10), 1928–1938, May (2011).

[54] Julienne, H., Zoufir, A., Audit, B., and Arneodo, A. Human genome replication proceeds through four chromatin states.

PLoS Com **9**, e1003233 (2013).

[55] Haddad, N., Vaillant, C., and Jost, D. Ic-finder: inferring robustly the hierarchical organization of chromatin folding. *Nucleic Acids Res* **45**, e81 (2017).

[56] Sexton, T., Yaffe, E., Kenigsberg, E., Bantignies, F., Leblanc, B., Hoichman, M., Parrinello, H., Tanay, A., and Cavalli, G. Three-dimensional folding and functional organization principles of the drosophila genome. *Cell* **148**(3), 458–472, Feb (2012).

[57] Imakaev, M., Fudenberg, G., McCord, R. P., Naumova, N., Goloborodko, A., Lajoie, B. R., Dekker, J., and Mirny, L. A. Iterative correction of hi-c data reveals hallmarks of chromosome organization. *Nat Methods* **9**(10), 999–1003, Oct (2012).

[58] Rowley, M. J., Nichols, M. H., Lyu, X., Ando-Kuri, M., Rivera, I. S. M., Hermetz, K., Wang, P., Ruan, Y., and Corces, V. G. Evolutionarily conserved principles predict 3d chromatin organization. *Molecular Cell* **67**, 837–852 (2017).

[59] Ulianov, S. V., Khrameeva, E. E., Gavrilov, A. A., Flyamer, I. M., Kos, P., Mikhaleva, E. A., Penin, A. A., Logacheva, M. D., Imakaev, M. V., Chertovich, A., Gelfand, M. S., Shevelyov, Y. Y., and Razin, S. V. Active chromatin and transcription play a key role in chromosome partitioning into topologically associating domains. *Genome Res* **26**(1), 70–84, Jan (2016).

[60] Olarte-Plata, J. D., Haddad, N., Vaillant, C., and Jost, D. The folding landscape of the epigenome. *Phys Biol* **13**(2), 026001 (2016).

[61] Rao, S. S., Huang, S.-C., St Hilaire, B. G., Engreitz, J. M., Perez, E. M., Kieffer-Kwon, K.-R., Sanborn, A. L., Johnstone, S. E., Bascom, G. D., Bochkov, I. D., et al. Cohesin loss eliminates all loop domains. *Cell* **171**, 305–320 (2017).

[62] Schwarzer, W., Abdennur, N., Goloborodko, A., Pekowska, A., Fudenberg, G., Loe-Mie, Y., Fonseca, N. A., Huber, W., Haering, C., Mirny, L., and Spitz, F. Two independent modes of chromosome organization are revealed by cohesin removal. *bioRxiv* **1**, 094185 (2016).

[63] Zhu, Y., Chen, Z., Zhang, K., Wang, M., Medovoy, D., Whitaker, J. W., Ding, B., Li, N., Zheng, L., and Wang, W. Constructing 3d interaction maps from 1d epigenomes. *Nat Commun* **7**, 10812 (2016).

[64] Fortin, J.-P. and Hansen, K. D. Reconstructing a/b compartments as revealed by hi-c using long-range correlations in epigenetic data. *Genome biology* **16**, 180 (2015).

[65] Pancaldi, V., Carrillo-de Santa-Pau, E., Javierre, B. M., Juan, D., Fraser, P., Spivakov, M., Valencia, A., and Rico, D. Integrating epigenomic data and 3d genomic structure with a new measure of chromatin assortativity. *Genome Biology* **17**, 152 (2016).

[66] Phillips-Cremins, J. E., Sauria, M. E. G., Sanyal, A., Gerasimova, T. I., Lajoie, B. R., Bell, J. S. K., Ong, C.-T., Hookway, T. A., Guo, C., Sun, Y., Bland, M. J., Wagstaff, W., Dalton, S., McDevitt, T. C., Sen, R., Dekker, J., Taylor, J., and Corces, V. G. Architectural protein subclasses shape 3d organization of genomes during lineage commitment. *Cell* **153**(6), 1281–1295, Jun (2013).

[67] Sofueva, S., Yaffe, E., Chan, W.-C., Georgopoulou, D., Vietri Rudan, M., Mira-Bontenbal, H., Pollard, S. M., Schroth, G. P., Tanay, A., and Hadjur, S. Cohesin-mediated interactions organize chromosomal domain architecture. *EMBO J* **32**(24), 3119–3129, Dec (2013).

[68] Whyte, W. A., Orlando, D. A., Hnisz, D., Abraham, B. J., Lin, C. Y., Kagey, M. H., Rahl, P. B., Lee, T. I., and Young, R. A. Master transcription factors and mediator establish super-enhancers at key cell identity genes. *Cell* **153**, 307–319 (2013).

[69] Funke, J. J., Ketterer, P., Lieleg, C., Schunter, S., Korber, P., and Dietz, H. Uncovering the forces between nucleosomes using dna origami. *Science Advances* **2**, e1600974 (2016).

[70] Bertin, A., Leforestier, A., Durand, D., and Livolant, F. Role of histone tails in the conformation and interactions of nucleosome core particles. *Biochemistry* **43**, 4773–4780 (2004).

[71] Jost, D., Carrivain, P., Cavalli, G., and Vaillant, C. Modeling epigenome folding: formation and dynamics of topologically

associated chromatin domains. *Nucleic Acids Res* **42**(15), 9553–9561 (2014).

[72] Haddad, N., Jost, D., and Vaillant, C. Perspectives: using polymer modeling to understand the formation and function of nuclear compartments. *Chromosome Research* **25**(1), 35, March (2017).

[73] Ghosh, S. K. and Jost, D. How epigenome drives chromatin folding and dynamics, insights from efficient coarse-grained models of chromosomes. *bioR* **1**, 200584 (2017).

[74] Bates, F. S. and Fredrickson, G. H. Block copolymer thermodynamics: theory and experiment. *Annual review of physical chemistry* **41**, 525–557 (1990).

[75] Hugouvieux, V., Axelos, M., and Kolb, M. Amphiphilic multiblock copolymers: From intramolecular pearl necklace to layered structures. *Macromolecules* **42**, 392–400 (2009).

[76] Rosa, A. and Everaers, R. Structure and dynamics of interphase chromosomes. *PLoS Comput. Biol.* **4**(8), e1000153 (2008).

[77] Mirny, L. A. The fractal globule as a model of chromatin architecture in the cell. *Chromosome Res* **19**(1), 37–51, Jan (2011).

[78] Doi, M. and Edwards, S. F. *The Theory of Polymer Dynamics*. Oxford University Press, New York, (1986).

[79] Naumova, N., Imakaev, M., Fudenberg, G., Zhan, Y., Lajoie, B. R., Mirny, L. A., and Dekker, J. Organization of the mitotic chromosome. *Science* **342**(6161), 948–953, Nov (2013).

[80] Caré, B., Emeriau, P.-E., Cortini, R., and Victor, J.-M. Chromatin epigenomic domain folding: size matters. *AIMS Biophysics* **2**, 517–530 (2015).

[81] Metz, C. W. Chromosome studies on the diptera. ii. the paired association of chromosomes in the diptera, and its significance. *Journal of Experimental Zoology Part A: Ecological Genetics and Physiology* **21**, 213–279 (1916).

[82] Rosa, A., Becker, N. B., and Everaers, R. Looping probabilities in model interphase chromosomes. *Biophys. J.* **98**, 2410–2419 (2010).

[83] Chen, H., Fujioka, M., and Gregor, T. Direct visualization of transcriptional activation by physical enhancer-promoter proximity. *bioRxiv* **1**, 099523 (2017).

[84] Di Pierro, M., Zhang, B., Lieberman-Aiden, E., Wolynes, P. G., and Onuchic, J. N. Transferable model for chromosome architecture. *Proc Natl Acad Sci U S A* **113**, 1216812173 (2016).

[85] Di Pierro, M., Cheng, R. R., Aiden, E. L., Wolynes, P. G., and Onuchic, J. N. De novo prediction of human chromosome structures: Epigenetic marking patterns encode genome architecture. *Proc Natl Acad Sci U S A* **114**, 1212612131 (2017).

[86] Liu, L., Shi, G., Thirumalai, D., and Hyeon, C. Architecture of human interphase chromosome determines the spatiotemporal dynamics of chromatin loci. *bioRxiv* **1**, 223669 (2017).

[87] Shi, G., Liu, L., Hyeon, C., and Thirumalai, D. Interphase human chromosome exhibits out of equilibrium glassy dynamics. *bioRxiv* **1**, 193375 (2017).

[88] Nuebler, J., Fudenberg, G., Imakaev, M., Abdennur, N., and Mirny, L. Chromatin organization by an interplay of loop extrusion and compartmental segregation. *bioRxiv* **1**, 196261 (2017).

[89] Barbieri, M., Chotalia, M., Fraser, J., Lavitas, L.-M., Dostie, J., Pombo, A., and Nicodemi, M. Complexity of chromatin folding is captured by the strings and binders switch model. *Proc Natl Acad Sci U S A* **109**(40), 16173–16178, Oct (2012).

[90] Barbieri, M., Xie, S. Q., Triglia, E. T., Chiariello, A. M., Bianco, S., de Santiago, I., Branco, M. R., Rueda, D., Nicodemi, M., and Pombo, A. Active and poised promoter states drive folding of the extended hoxb locus in mouse embryonic stem cells. *Nature Structural & Molecular Biology* **24**, 515524 (2017).

[91] Chiariello, A. M., Annunziatella, C., Bianco, S., Esposito, A., and Nicodemi, M. Polymer physics of chromosome large-scale 3d organisation. *Sci Rep* **6**, 29775 (2016).

[92] Brackley, C. A., Johnson, J., Kelly, S., Cook, P. R., and Marenduzzo, D. Simulated binding of transcription factors to active and inactive regions folds human chromosomes into loops, rosettes and topological domains. *Nucleic Acids Res*

44(8), 3503–3512, May (2016).

[93] Brackley, C. A., Brown, J. M., Waithe, D., Babbs, C., Davies, J., Hughes, J. R., Buckle, V. J., and Marenduzzo, D. Predicting the three-dimensional folding of cis-regulatory regions in mammalian genomes using bioinformatic data and polymer models. *Genome Biology* **17**, 59 (2016).

[94] Brackley, C. A., Liebchen, B., Michieletto, D., Mouvet, F., Cook, P. R., and Marenduzzo, D. Ephemeral protein binding to dna shapes stable nuclear bodies and chromatin domains. *Biophysical Journal* **112**, 1085–1093 (2017).

[95] Awazu, A. Nuclear dynamical deformation induced hetero-and euchromatin positioning. *Phys Rev E* **92**, 032709 (2015).

[96] Smrek, J. and Kremer, K. Small activity differences drive phase separation in active-passive polymer mixtures. *Phys Rev Lett* **118**, 098002 (2017).

[97] Ganai, N., Sengupta, S., and Menon, G. I. Chromosome positioning from activity-based segregation. *Nucleic Acids Res* **42**(7), 4145–4159, Apr (2014).

[98] Iborra, F. J. Can visco-elastic phase separation, macromolecular crowding and colloidal physics explain nuclear organisation? *Theoretical Biology and Medical Modelling* **4**, 15 (2007).

[99] Lee, S. S., Tashiro, S., Awazu, A., and Kobayashi, R. A new application of the phase-field method for understanding the mechanisms of nuclear architecture reorganization. *Journal of mathematical biology* **74**, 333–354 (2017).

[100] Oehler, S. and Mller-Hill, B. High local concentration: A fundamental strategy of life. *J. Mol. Biol.* **395**, 242–253 (2010).

[101] Vilar, J. and Leibler, S. Dna looping and physical constraints on transcription regulation. *J Mol Biol* **331**, 981–989 (2003).

[102] Spitz, F. Gene regulation at a distance: from remote enhancers to 3d regulatory ensembles. *Semin Cell Dev Biol* **57**, 57–67 (2016).

[103] Lanzuolo, C., Roure, V., Dekker, J., Bantignies, F., and Orlando, V. Polycomb response elements mediate the formation of chromosome higher-order structures in the bithorax complex. *Nat Cell Biol* **9**, 1167–1174 (2007).

[104] Wani, A. H., Boettiger, A. N., Schorderet, P., Ergun, A., Münger, C., Sadreyev, R. I., Zhuang, X., Kingston, R. E., and Francis, N. J. Chromatin topology is coupled to polycomb group protein subnuclear organization. *Nat Commun* **7**, 10291 (2016).

[105] Vieux-Rochas, M., Fabre, P., Leleu, M., Duboule, D., and Noordermeer, D. Clustering of mammalian hox genes with other h3k27me3 targets within an active nuclear domain. *Proc Natl Acad Sci U S A* **112**, 4672–4677 (2015).

[106] Bantignies, F., Roure, V., Comet, I., Leblanc, B., Schuettengruber, B., Bonnet, J., Tixier, V., Mas, A., and Cavalli, G. Polycomb-dependent regulatory contacts between distant hox loci in drosophila. *Cell* **144**(2), 214–226, Jan (2011).

[107] Meister, P. and Taddei, A. Building silent compartments at the nuclear periphery: a recurrent theme. *Curr Opin Genet Dev* **23**, 96–103 (2013).

[108] Dily, F. L., Ba, D., Pohl, A., Vicent, G. P., Serra, F., Soronellas, D., Castellano, G., Wright, R. H. G., Ballare, C., Filion, G., Marti-Renom, M. A., and Beato, M. Distinct structural transitions of chromatin topological domains correlate with coordinated hormone-induced gene regulation. *Genes Dev* **28**(19), 2151–2162, Oct (2014).

[109] Giorgetti, L., Galupa, R., Nora, E. P., Piolot, T., Lam, F., Dekker, J., Tiana, G., and Heard, E. Predictive polymer modeling reveals coupled fluctuations in chromosome conformation and transcription. *Cell* **157**, 950–963 (2014).

[110] Al-Sady, B., Madhani, H., and Narlikar, G. Division of labor between teh chromodomains of HP1 and Suv39 methylase enables coordination of heterochromatin spread. *Mol Cell* **51**, 80–91 (2013).

[111] Yuan, W., Wu, T., Fu, H., Dai, C., Wu, H., Liu, N., Li, X., Xu, M., Zhang, Z., and al. Dense chromatin activates Polycomb repressive complex 2 to regulate h3 lysine 27 methylation. *Science* **337**, 971–975 (2012).

[112] Lavigne, M., Francis, N., King, I., and Kingston, R. Propagation of silencing; recruitment and repression of naive chromatin in trans by polycomb repressed chromatin. *Mol C* **13**, 415–425 (2004).

[113] Obersriebnig, M. J., Pallesen, E. M. H., Sneppen, K., Trusina, A., and Thon, G. Nucleation and spreading of a hete-

rochromatic domain in fission yeast. *Nat Commun* **7**, 11518 (2016).

[114] Sharma, R., Jost, D., Kind, J., Gmez-Saldivar, G., van Steensel, B., Askjaer, P., Vaillant, C., and Meister, P. Differential spatial and structural organization of the x chromosome underlies dosage compensation in c. elegans. *Genes Dev* **28**(23), 2591–2596, Dec (2014).

[115] Dodd, I. B., Micheelsen, M. A., Sneppen, K., and Thon, G. Theoretical analysis of epigenetic cell memory by nucleosome modification. *Cell* **129**(4), 813–822, May (2007).

[116] Angel, A., Song, J., Dean, C., and Howard, M. A polycomb-based switch underlying quantitative epigenetic memory. *Nature* **476**, 105–108 (2011).

[117] Jost, D. Bifurcation in epigenetics: implications in development, proliferation, and diseases. *Phys Rev E Stat Nonlin Soft Matter Phys* **89**(1), 010701, Jan (2014).

[118] Dayarian, A. and Sengupta, A. Titration and hysteresis in epigenetic chromatin silencing. *Phys* **10**, 036005 (2013).

[119] Erdel, F. and Greene, E. C. Generalized nucleation and looping model for epigenetic memory of histone modifications. *Proceedings of the National Academy of Sciences* **113**, E4180–E4189 (2016).

[120] Sneppen, K. and Dodd, I. Cooperative stabilization of the SIR complex provides robust epigenetic memory in a model of SIR silencing in Saccharomyces cerevisiae. *Epigenetics* **10**(4), 293–302 (2015).

[121] Berry, S., Dean, C., and Howard, M. Slow chromatin dynamics allow polycomb target genes to filter fluctuations in transcription factor activity. *Cell Systems* **4**, 1–13 (2017).

[122] Jost, D. and Vaillant, C. Epigenomics in 3d: importance of long-range spreading and speci c interactions in epigenomic maintenance. *Nucleic Acids Res* **In press** (2018).

[123] Zerihun, M. B., Vaillant, C., and Jost, D. Effect of replication on epigenetic memory and consequences on gene transcription. *Phys Biol* **12**(2), 026007, Apr (2015).

[124] Grosberg, A. Y. Disordered polymers. *Physics-Uspekhi* **40**, 125–158 (1997).

[125] Grosberg, A. Y. and Khokhlov, A. R. *Statistical physics of macromolecules*. AIP Press, (1994).

[126] Mukamel, D., Ruffo, S., and Schreiber, N. Breaking of ergodicity and long relaxation times in systems with long-range interactions. *Phys Rev Lett* **95**, 240604 (2005).

[127] Laprell, F., Finkll, K., and J., M. Propagation of Polycomb-repressed chromatin requires sequence-specific recruitment to DNA. *Science* **356**, 85–88 (2017).

[128] Wang, X. and Moazed, D. Dna seuence-dependent epigenetic inheritance of gene silencing and histone H3K9 methylation. *Science* **356**, 88–91 (2017).

[129] Coleman, R. and Struhl, G. Causal role for inheritance of H3K27me3 in maintaining the OFF state of a *drosophila* HOX gene. *Science* **356**, eaai8236 (2017).

[130] Schuettengruber, B., Elkayam, N. O., Sexton, T., Entrevan, M., Stern, S., Thomas, A., Yaffe, E., Parrinello, H., Tanay, A., and Cavalli, G. Cooperativity, specificity, and evolutionary stability of Polycomb targeting in Drosophila. *Cell Rep* **9**, 219–233 (2014).

[131] Sneppen, K. and Mitarai, N. Multistability with a metastable mixed state. *Phys Rev Lett* **109**, 100602 (2012).

[132] Michieletto, D., Orlandini, E., and Marenduzzo, D. Polymer model with epigenetic recoloring reveals a pathway for the de novo establishment and 3d organization of chromatin domains. *Phys Rev X* **6**, 041047 (2016).

[133] Jerabek, H. and Heermann, D. W. How chromatin looping and nuclear envelope attachment affect genome organization in eukaryotic cell nuclei. *Int Rev Cell Mol Biol* **307**, 351–381 (2014).

[134] Sexton, T. and Cavalli, G. The role of chromosome domains in shaping the functional genome. *Cell* **160**(6), 1049–1059, Mar (2015).

[135] Tolhuis, B., Blom, M., Kerkhoven, R. M., Pagie, L., Teunissen, H., Nieuwland, M., Simonis, M., de Laat, W., van Lohuizen, M., and van Steensel, B. Interactions among polycomb domains are guided by chromosome architecture. *PLoS*

Genet **7**(3), e1001343, Mar (2011).

[136] Waddington, C. H. *The strategy of the genes*, volume 20. Routledge, (2014).